SECURITY CLASSIFICATION OF THIS PAGE *(When Data Entered)*

| REPORT DOCUMENTATION PAGE | | READ INSTRUCTIONS BEFORE COMPLETING FORM |
|---|---|---|
| 1. REPORT NUMBER<br>NRL Report 7835 | 2. GOVT ACCESSION NO. | 3. RECIPIENT'S CATALOG NUMBER |
| 4. TITLE *(and Subtitle)*<br>MATHEMATICAL ANALYSIS OF CURRENT DISTRIBUTION IN CORROSION CELLS WITH CIRCULAR GEOMETRY | | 5. TYPE OF REPORT & PERIOD COVERED<br>Final report on one phase of the NRL problem<br>6. PERFORMING ORG. REPORT NUMBER |
| 7. AUTHOR*(s)*<br>E. McCafferty | | 8. CONTRACT OR GRANT NUMBER*(s)* |
| 9. PERFORMING ORGANIZATION NAME AND ADDRESS<br>Naval Research Laboratory<br>Washington, D.C. 20375 | | 10. PROGRAM ELEMENT, PROJECT, TASK AREA & WORK UNIT NUMBERS<br>NRL Problem M04-09;<br>Project RR 022-08-44-5513 |
| 11. CONTROLLING OFFICE NAME AND ADDRESS<br>Department of the Navy<br>Office of Naval Research<br>Arlington, VA 22217 | | 12. REPORT DATE<br>January 31, 1975<br>13. NUMBER OF PAGES<br>40 |
| 14. MONITORING AGENCY NAME & ADDRESS*(if different from Controlling Office)* | | 15. SECURITY CLASS. *(of this report)*<br>Unclassified<br>15a. DECLASSIFICATION/DOWNGRADING SCHEDULE |

16. DISTRIBUTION STATEMENT *(of this Report)*

Approved for public release; distribution unlimited.

17. DISTRIBUTION STATEMENT *(of the abstract entered in Block 20, if different from Report)*

18. SUPPLEMENTARY NOTES

19. KEY WORDS *(Continue on reverse side if necessary and identify by block number)*

Corrosion
Current distribution
Potential distribution
Thin layers
Circular electrodes

20. ABSTRACT *(Continue on reverse side if necessary and identify by block number)*

The distribution of current in a corrosion cell with circular geometry has been computed on the assumption that the electrolyte has a uniform composition, so that potential distribution is given by Laplace's equation. The current distribution is more uniform along the metal surface under bulk electrolyte than under thin layers of electrolyte. For thin layers, there is a geometry effect in which corrosion attack is intensified at the anode/cathode boundary. For a fixed anode radius, this local attack is promoted by decreasing the electrolyte thickness or linear polarization parameter or by increasing the cathode radius.

DD FORM 1 JAN 73 1473 EDITION OF 1 NOV 65 IS OBSOLETE
S/N 0102-014-6601 |



SECURITY CLASSIFICATION OF THIS PAGE *(When Data Entered)*

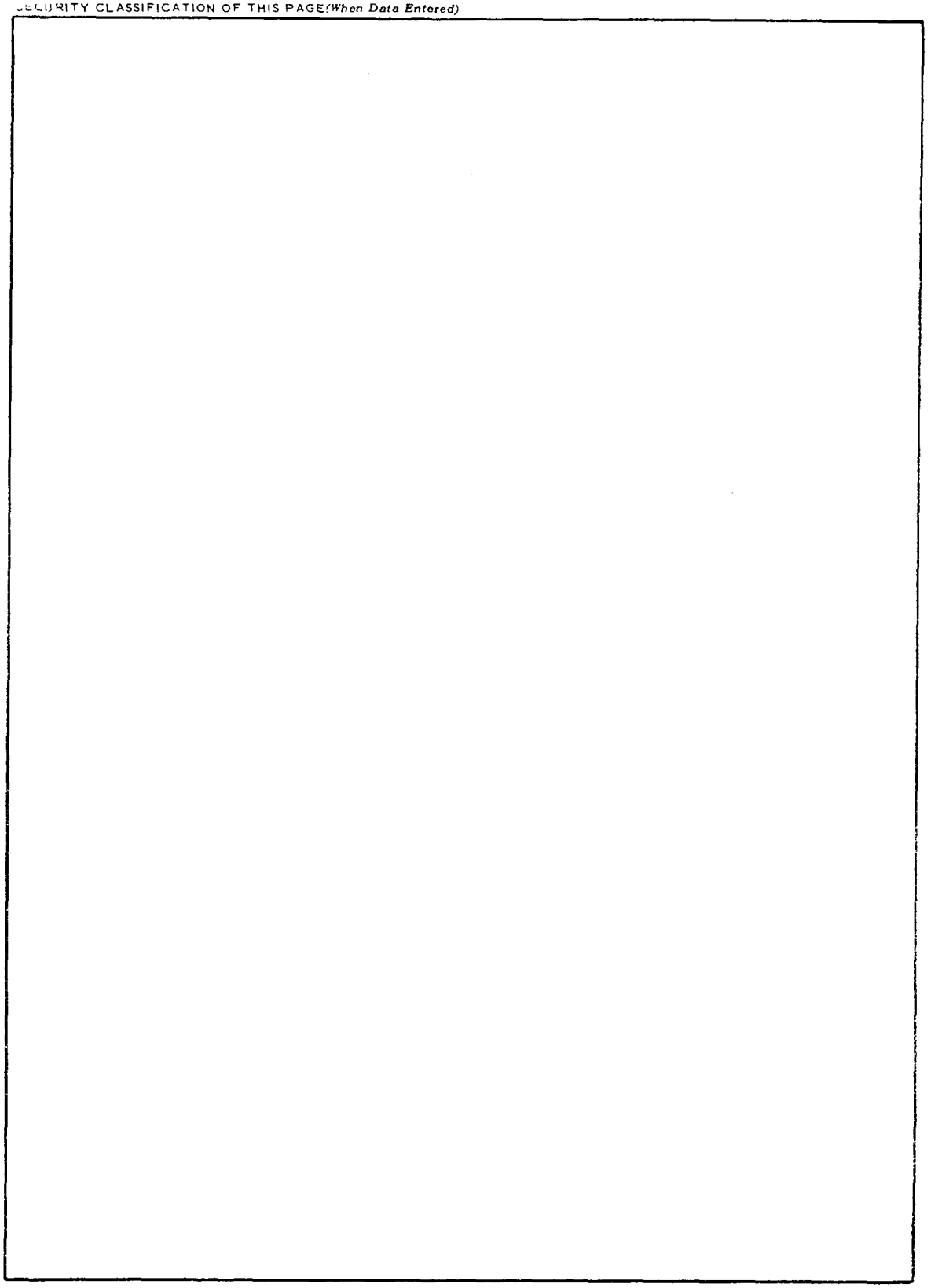

CONTENTS

# MATHEMATICAL ANALYSIS OF CURRENT DISTRIBUTION IN CORROSION CELLS WITH CIRCULAR GEOMETRY

## INTRODUCTION

In the case of uniform corrosion, existent local anodes and cathodes are distributed randomly over the surface, and their individual locations fluctuate with time. In this situation, the electrode has a "mixed" potential [1] which, like the current density, is uniform throughout the metal surface.

In many cases, however, anodic and cathodic reactions occur on different surfaces, as in the galvanic corrosion of dissimilar metals, or on different parts of the same surface, as with localized geometries such as corrosion pits or crevices. In these instances, there is a varying distribution of both current and potential over the metal surface.

Waber and coworkers [2 - 6] have treated the current distribution in systems where the anode and cathode are coplanar, parallel strips of infinite length. This method of calculation has been extended recently to two-dimensional geometries for coplanar, concentric rectangles [7] and circles [8].

In the case of circular geometries, Gal-Or, Raz, and Yahalom [8] have calculated the *total* current between coplanar electrodes under a thin layer of electrolyte, although these authors did not evaluate the *local* current along the cell radius. In many instances of localized corrosion, the corroding metal has a circular geometry. Examples include some instances of pitting [9], corrosion under tubercules on copper [10], and crevice corrosion under O-rings or washers [11]. Thus it would be useful to map the corrosion current distribution in systems of circular geometry.

The purpose of this report is thus to supplement the recent work of Gal-Or and coworkers [8] by evaluating the distribution of current and potential in systems of circular electrodes as a function of variable cell dimensions and linear polarization parameters. Both bulk electrolyte and thin-electrolyte layers will be considered.

## MATHEMATICAL BACKGROUND

The mathematical method used by Waber and coworkers [2 - 6] is well known. This section will sketch the elements of that method. The paper by Gal-Or and coworkers [8] gives a detailed account of their solution for the particular case of circular electrodes covered by a thin layer of electrolyte. The derivation for concentric circular electrodes under bulk electrolyte has not been published, although the derivation is quite similar to the thin-layer case. The equation for the bulk case will be derived in this report for completeness. It will be seen that the current distribution for bulk electrolyte is the limiting case for thin layers.

Manuscript submitted October 17, 1974.

## Potential Distribution

The following will apply to a generalized geometry in which the electrode surfaces are placed in the $XY$ plane, as shown in Fig. 1. No specific geometry is yet assumed.

The central assumption is that the electrostatic potential $P$ at any point in the electrolyte is given by Laplace's equation

$$\frac{\partial^2 P}{\partial x^2} + \frac{\partial^2 P}{\partial y^2} + \frac{\partial^2 P}{\partial z^2} = 0. \tag{1}$$

Laplace's equation is valid if the following conditions are met:

(1) There are no concentration gradients in the electrolyte (uniform composition).

(2) The solution is electroneutral.

(3) There are no sources or sinks of ions in the bulk electrolyte.

For more detail see Ref. 12. To solve Eq. (1), one must solve a boundary-value problem for which the potential is specified at the boundaries of the electrolyte, including the electrode surface.

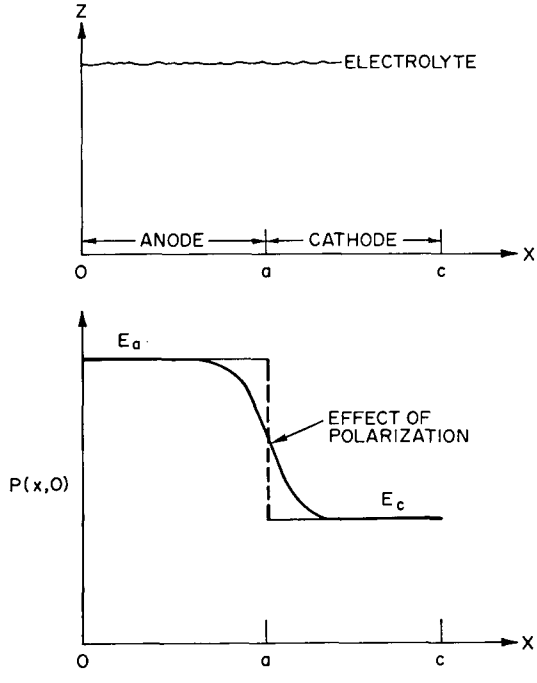


Fig. 1—Coordinate system and electrode potentials along the metal surface ($y$ = constant, $z = 0$)

### Current Density

The current density $i(A/cm^2)$ at any point in the electrolyte is related to the potential by

$$i = -\sigma \frac{\partial P}{\partial n}, \tag{2}$$

where $\sigma$ is the solution conductivity ($ohm^{-1}cm^{-1}$) and $\partial P/\partial n$ is the normal gradient of the potential ($v\ cm^{-1}$) in the direction of the interior of the electrolyte. At the electrode surface ($z = 0$),

$$i(x, 0) = -\sigma \left[\frac{\partial P(x, z)}{\partial z}\right]_{z=0}. \tag{3}$$

Thus when Laplace's equation is solved for $P(x, z)$, the corrosion current distribution follows from Eq. (3).

### Linear Polarization

Waber [2 - 6], following Wagner [13], assumed linear polarization, that is, that plots of current density vs electrode potential are linear. This assumption, intended to simplify the mathematics, is a reasonable approximation in a number of cases.

Figure 1 also shows the potential distribution along the electrode surfaces; $E_a$ and $E_c$ are the potentials of the unpolarized anode and cathode respectively. Figure 2 shows the corresponding linear polarization curves. The slope of the cathodic branch is

$$\text{slope} = \frac{di(x, 0)}{dP(x, 0)} = \frac{i(x, 0) - 0}{P(x, 0) - E_c}.$$

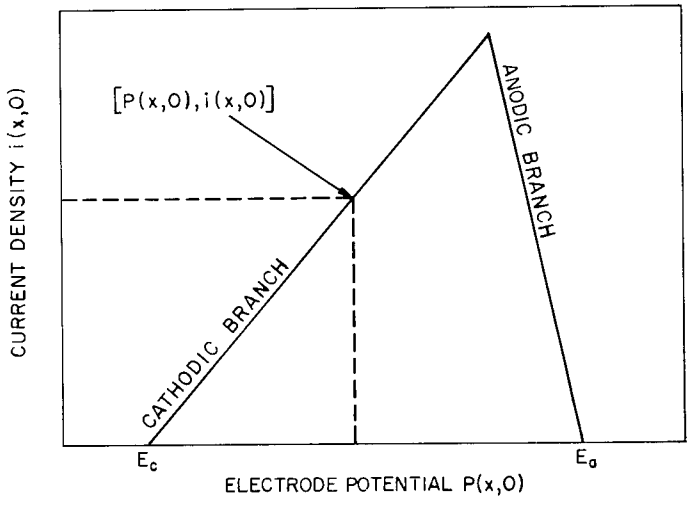


Fig. 2—Linear polarization curves, $y$ = constant (schematic)

Rearranging,

$$P(x, 0) - i(x, 0)\frac{dE}{di} = E_c , \tag{4}$$

where we have written the simpler (and more conventional) notation $dE/di$ for $dP(x, 0)/di(x, 0)$, the slope of the linear polarization curve. Use of Eq. (3) for $i(x, 0)$ in Eq. (4) gives

$$P(x, 0) - \left\{-\sigma\left[\frac{\partial P(x, z)}{\partial z}\right]_{z=0} \cdot \frac{dE}{di}\right\} = E_c . \tag{5}$$

The Wagner polarization parameter $\mathfrak{L}$ is defined [2, 13] as

$$\mathfrak{L} \equiv \sigma\left|\frac{dE}{di}\right|, \tag{6}$$

where $\mathfrak{L}$ has the dimensions of length. Use of Eq. (6) in Eq. (5) gives

$$P(x, 0) - \mathfrak{L}_c\left[\frac{\partial P(x, z)}{\partial z}\right]_{z=0} = E_c . \tag{7}$$

A similar equation holds for the anodic branch:

$$P(x, 0) - \mathfrak{L}_a\left[\frac{\partial P(x, z)}{\partial z}\right]_{z=0} = E_a . \tag{8}$$

If both branches of the polarization curve have the same slope, $\mathfrak{L}_a = \mathfrak{L}_c = \mathfrak{L}$, and

$$P(x, 0) - \mathfrak{L}\left[\frac{\partial P(x, z)}{\partial z}\right]_{z=0} = S(x) , \tag{9}$$

where

$$S(x) = \begin{cases} E_a, & 0 \leqslant x < a ; \\ E_c, & a < x \leqslant c . \end{cases}$$

Figure 3 shows an example of polarization data [14] which give good linear plots. When the current is plotted in the usual logarithmic way, the cathodic curve is seen to be typical of a diffusion-controlled process, whereas the anodic curve is typical of activation-controlled dissolution. Yet both curves are linear in current in the millampere range as the short-circuited potential is approached.

Tables 1 and 2 list a variety of systems which have been observed to display linear polarization curves over at least a portion, if not the entirety, of current range. Thus the mathematical assumption of linear polarization is not always unrealistic. More serious, however, is the added assumption that the anodic and cathodic linear polarization parameters are equal.

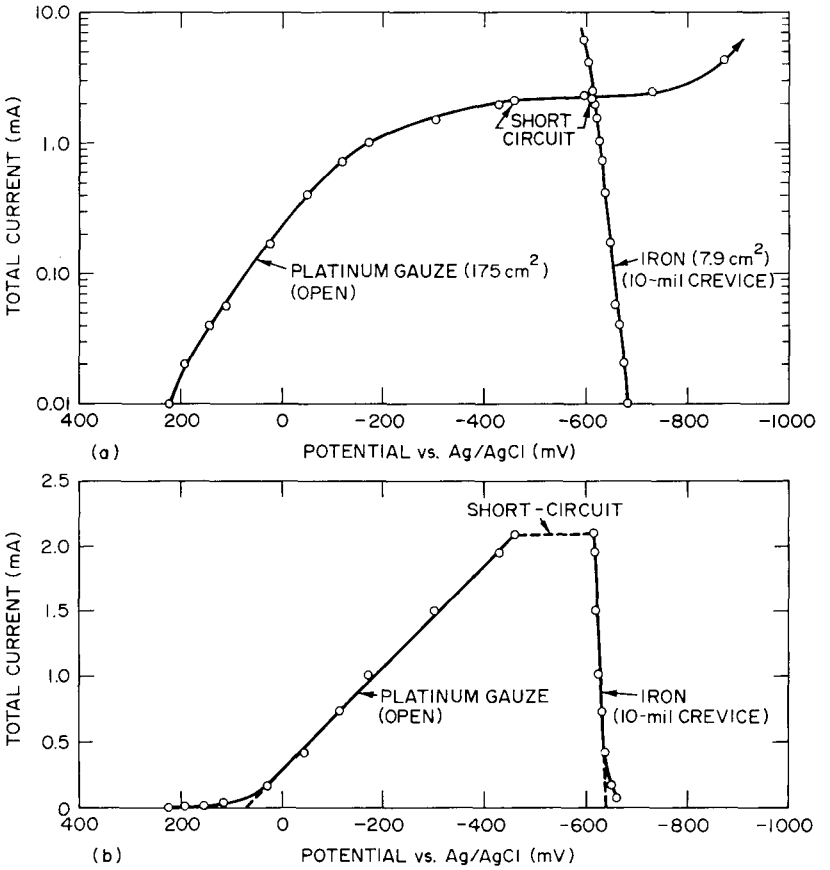


Fig. 3—Potentiostatic polarization of iron (10-mil crevice) and platinum (open) in 0.06N NaCl (a) Plotted semilogarithmically (b) Plotted linearly

Values of the anodic linear polarization parameters $\mathfrak{L}_a$ compiled in Table 1 range from 0 to 5 cm. Values of the cathodic parameter $\mathfrak{L}_c$ in Table 2 range from approximately 0.2 to 250 cm. Comparison of $\mathfrak{L}_a$ and $\mathfrak{L}_c$ for a given system shows that $\mathfrak{L}_c$ is generally larger. Thus the assumption that $\mathfrak{L}_a = \mathfrak{L}_c$ is generally not valid.

However, in the case of a partially restrictive third dimension, such as a crevice above the anode, $\mathfrak{L}_a$ and $\mathfrak{L}_c$ are probably closer to each other than for totally open geometries. With localized geometries, as in crevices or pits, it is well known that the local corrodent has a different composition than the bulk solution [17, 18]. Thus the conductivity $\sigma$ used to calculate $\mathfrak{L}$ should be that of the internal electrolyte. In the case of iron, the internal electrolyte of a macro facsimile of an iron crevice or pit modeled according to thermodynamic reasoning [19] has been found to be approximately 4M in $FeCl_2$ [20]. For 0.1N NaCl, for instance, the anolyte conductivity $\sigma_a$ would be approximately ten times that of the bulk catholyte conductivity $\sigma_c$ [21]. These considerations would tend to bring anodic and cathodic values of $\mathfrak{L}$ into closer agreement.

TABLE 1
Selected Values of Anodic Linear Polarization Parameters $\mathfrak{L}_a$

| Metal | Solution | Solution Thickness | $\mathfrak{L}_a$ (cm) | Region of Linearity | Source |
|---|---|---|---|---|---|
| Iron | 0.06N NaCl | 10-mil crevice (254 $\mu$m) | 0.75 | See Fig. 3 | Fig. 3 |
| | 0.1N NaCl | bulk<br>70 $\mu$m | 0<br>1.3 | $i > 100\ \mu A/cm^2$<br>$i > 150$ | Calculated from the data of Rosenfeld [15] |
| Zinc | 0.1N NaCl | bulk<br>165 $\mu$m | 0.80<br>0.80 | $i > 50\ \mu A/cm^2$<br>$i > 75$ | Calculated from the data of Rosenfeld [15] |
| | 20% $CrO_3$ | bulk | 1.12 - 3.12 | — | Compiled by Waber [16] |
| Magnesium | 0.1N NaCl | bulk<br>70 $\mu$m<br>165 $\mu$m | 0.32<br>0.91<br>0.43 | $i > 50\ \mu A/cm^2$<br>$i > 100$<br>$i > 50$ | Calculated from data of Rosenfeld [15] |
| Copper | 1M $Cu(Cl0_4)_2$ | bulk | 0.3 | — | Compiled by Waber [16] |
| Steel | 0.01N NaBr (pH = 2.2) | bulk | 0.80 | $i < 1\ mA/cm^2$ | Gal-Or, Raz, and Yaholom [8] |

TABLE 2
Selected Values of Cathodic Linear Polarization Parameters $\mathfrak{L}_c$

| Metal | Solution | Solution Thickness | $\mathfrak{L}_c$ (cm) | Region of Linearity | Source |
|---|---|---|---|---|---|
| Iron | 0.1N NaCl | bulk | 92 | $i < 75\ \mu A/cm^2$ | Calculated from data of Rosenfeld [15] |
| | | | 3.1 | $i > 100$ | |
| | | 100 $\mu$m | 22 | $i > 100$ | |
| Zinc | 0.1N NaCl | bulk | 79 | $i < 50\ \mu A/cm^2$ | Calculated from data of Rosenfeld [15] |
| | | | 3.1 | $i > 100$ | |
| | | 100 $\mu$m | 11 | $i > 100$ | |
| | 0.05N KCl | bulk | 0.718 | — | Compiled by Waber [16] |
| | 0.2N $KClO_3$ | bulk | 0.21 | — | Compiled by Waber [16] |
| Magnesium | 0.1N NaCl | bulk | 0.64 | $i < 125\ \mu A/cm^2$ | Calculated from data of Rosenfeld [15] |
| | | | 2.2 | $i > 125$ | |
| | | 100 $\mu$m | 6.3 | $i > 100$ | |
| Copper | 0.1N NaCl | bulk | 81 | $i < 150\ \mu A/cm^2$ | Calculated from data of Rosenfeld [15] |
| | | 165 $\mu$m | 44 | $i < 250$ | |
| Platinum | 0.06N NaCl | bulk | 239 | See Fig. 3 | Fig. 3 |

Thus the assumption that anodic and cathodic linear polarization parameters are equal, though not necessarily valid, does simplify the mathematics to allow a first estimate of current and potential distributions within corrosion cells.

## BULK ELECTROLYTE

### Mathematical Analysis

The cell geometry is shown in Fig. 4. The anode and cathode edges are coplanar circles of radii $a$ and $c$ respectively. With the circular geometry, it is convenient to recast the Laplace equation

$$\frac{\partial^2 P}{\partial x^2} + \frac{\partial^2 P}{\partial y^2} + \frac{\partial^2 P}{\partial z^2} = 0 \tag{1}$$

in cylindrical coordinates through the usual relations

$$\begin{aligned} x &= r\cos\theta \\ y &= r\sin\theta \\ z &= z\,. \end{aligned} \tag{10}$$

The result is

$$\frac{\partial^2 P}{\partial r^2} + \frac{1}{r}\cdot\frac{\partial P}{\partial r} + \frac{\partial^2 P}{\partial z^2} = 0, \tag{11}$$

with the term in $\partial^2 P/\partial\theta^2$ deleted because the potential is not dependent on the angle $\theta$. The general approach is to

- solve Eq. (11) for $P(r, z)$ subject to the appropriate boundary conditions, which will be listed below,

and then to

- evaluate the local current density $i(r, 0)$ at the electrode surface using Eq. (3) in the form

$$i(r, 0) = -\sigma\left[\frac{\partial P(r, z)}{\partial z}\right]_{z=0}. \tag{12}$$

We next list the appropriate boundary conditions:

*Boundary condition 1:* No current flows parallel to the metal surface across the terminal edge of the cathode ($r = c$). Then

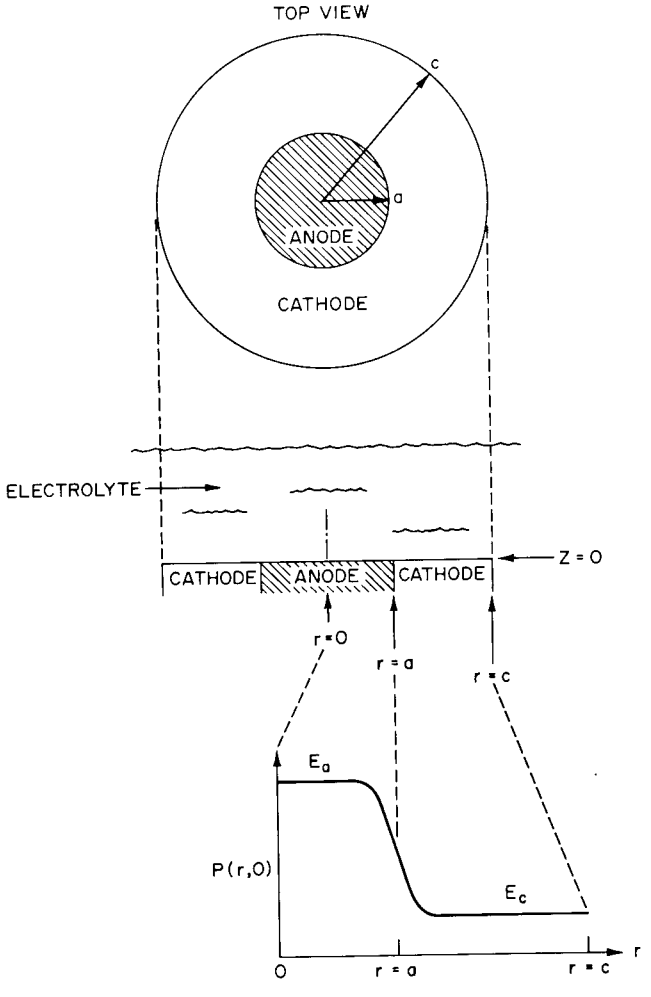


Fig. 4—Cell geometry and electrode potentials

$$i(r, c) = -\sigma \left[\frac{\partial P(r, z)}{\partial r}\right]_{r=c} = 0 , \tag{13}$$

or

$$\left[\frac{\partial P(r, z)}{\partial r}\right]_{r=c} = 0 . \tag{14}$$

*Boundary condition 2:* No current flows across the symmetry line $r = 0$*:

$$\left[\frac{\partial P(r, z)}{\partial r}\right]_{r=0} = 0 \tag{15}$$

*This boundary condition is required to make $P(r, z)$ bounded at $r = 0$. Alternately we could write the boundary condition as $\lim_{r \to 0} P(r, z) < L$, where $L$ is finite.

The physical interpretation is that electrons lost in the anodic reaction migrate to the nearest cathodic region rather than taking the longer path across the line $r = 0$.

*Boundary condition 3:* The potential $P(r, z)$ must be bounded at the upper physical boundary of the electrolyte, that is,

$$\lim_{z\to\infty} P(r, z) < M , \tag{16}$$

where $M$ is some finite number.*

*Boundary conditon 4:* The final boundary condition describes the potential at the electrode surfaces and is given by Eq. (8) in terms of $r$:

$$P(r, 0) - \mathfrak{L}\left[\frac{\partial P(r, z)}{\partial z}\right]_{z=0} = S(r) , \tag{17}$$

where

$$S(r) = \begin{cases} E_a, & 0 \leqslant r < a ; \\ E_c, & a < r \leqslant c . \end{cases} \tag{18}$$

The solution to Laplace's equation in cylindrical coordinates, that is, Eq. (11) subject to boundary conditions 1 through 4, is

$$P(r, z) = \left(\frac{a}{c}\right)^2 E_a + \left(\frac{c^2 - a^2}{c^2}\right) E_c + (E_a - E_c) \sum_{n=1}^{\infty} \frac{\frac{2}{x_n} \frac{a}{c} J_1\left(x_n \frac{a}{c}\right)}{\left(1 + \frac{\mathfrak{L}}{c} x_n\right) \left[J_0(x_n)\right]^2} e^{-x_n z/c} J_0\left(x_n \frac{r}{c}\right) , \tag{19}$$

where $E_a$ and $E_c$ are the potentials of the unpolarized anode and cathode, $J_0$ and $J_1$ are Bessel functions of order zero and one respectively, and the $x_n$ are the roots of $J_1(x)$ which give $J_1(x) = 0$. A detailed derivation of Eq. (19) is given in Appendix A. Along the electrode surface, the potential variation with radial distance is thus

$$P(r, 0) = \left(\frac{a}{c}\right)^2 E_a + \left(\frac{c^2 - a^2}{c^2}\right) E_c + (E_a - E_c) \sum_{n=1}^{\infty} \frac{\frac{2}{x_n} \left(\frac{a}{c}\right) J_1\left(x_n \frac{a}{c}\right)}{\left(1 + \frac{\mathfrak{L}}{c} x_n\right) \left[J_0(x_n)\right]^2} J_0\left(x_n \frac{r}{c}\right) . \tag{20}$$

We next evaluate the current distribution along the metal surface from

$$i(r, 0) = -\sigma\left[\frac{\partial P(r, z)}{\partial z}\right]_{z=0} . \tag{12}$$

*Alternately, there is no current flow across the upper boundary of the electrolyte.

Differentiation of Eq. (19) gives

$$i(r, 0) = 2\frac{\sigma}{c}(E_a - E_c)\sum_{n=1}^{\infty}\frac{\frac{a}{c}J_1\left(x_n\frac{a}{c}\right)}{\left(1 + \frac{\mathfrak{L}}{c}x_n\right)\left[J_0(x_n)\right]^2}J_0\left(x_n\frac{r}{c}\right), \tag{21}$$

or

$$\frac{i(r, 0)}{2\frac{\sigma}{c}(E_a - E_c)} = \sum_{n=1}^{\infty}\frac{\frac{a}{c}J_1\left(x_n\frac{a}{c}\right)}{\left(1 + \frac{\mathfrak{L}}{c}x_n\right)\left[J_0(x_n)\right]^2}J_0\left(x_n\frac{r}{c}\right). \tag{22}$$

The left-hand side of Eq. (22) is dimensionless and may be termed the "dimensionless local current density" $i^*$:

$$i^* \equiv \frac{i(r, 0)}{2\frac{\sigma}{c}(E_a - E_c)}. \tag{23}$$

Thus the current distribution depends only on the cell dimensions $a$ and $c$ and on the polarization parameter $\mathfrak{L}$ or, more properly, on the "reduced" radius $r/c$, the "reduced" cell dimension $a/c$, and on the "reduced" polarization parameter $\mathfrak{L}/c$.

### Numerical Evaluation

Figure 5 shows the dimensionless local current density $i^*$ as a function of reduced polarization parameter $\mathfrak{L}/c$ for a fixed cell configuration of $a/c = 0.5$. The points in Fig. 5 were computed using Eq. (22) with $n = 500$, except near $r/c = 0$ and $r/c$ near 0.5, where 2000 terms were needed for sharp convergence. The computer program used in the evaluation is given in Appendix B.

As seen in Fig. 5, the local current density is uniform across the cell for the larger values of $\mathfrak{L}$, and there is only a slight increase in corrosion current density at the anode/cathode junction for the smallest $\mathfrak{L}$ considered.

The corresponding potential distributions are given in Fig. 6. Potentials were calculated from Eq. (20) with $E_c$ taken to be 0; $n = 100$ sufficed to evaluate the sum. Figure 6 shows the potential is uniform across the cell for $\mathfrak{L}/c = 100$, nearly uniform for $\mathfrak{L}/c = 10$, and not uniform for $\mathfrak{L}/c = 1$.

For a given electrolyte (fixed conductivity $\sigma$), the larger $\mathfrak{L}$ corresponds to a larger value of $dE/di$: $\mathfrak{L} = \sigma|dE/di|$. Thus the larger $\mathfrak{L}$ means a more polarizable electrode, that is, a greater change in potential for a given current, as shown in Fig. 7.

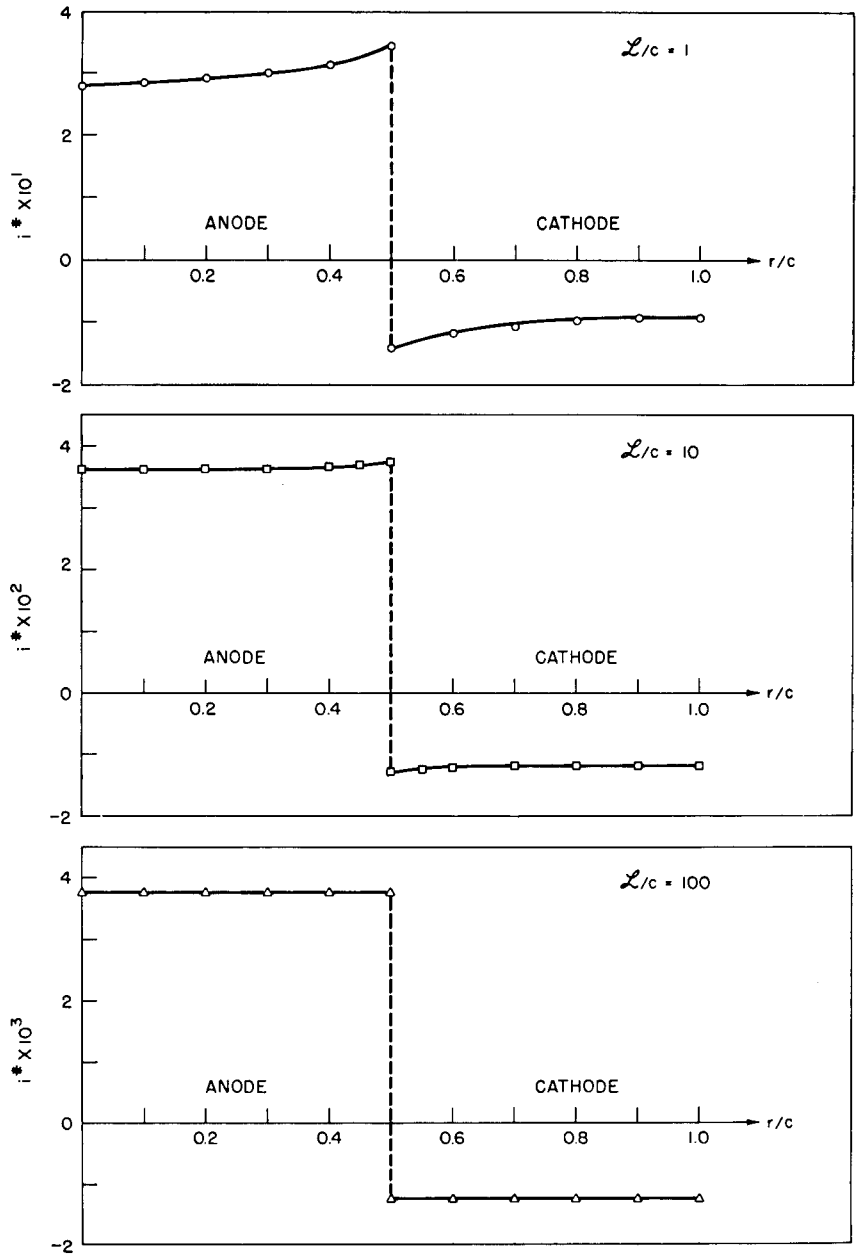


Fig. 5—Current distribution under bulk electrolyte for different polarization parameters at a fixed cell size ($a/c$ = 0.5)

Thus Figs. 5 and 6 show that the more polarizable the electrode system, the more uniform the distribution of potential and current. That is, the effect of coupling such electrodes is to distribute the polarization effect throughout the corrosion cell. For the least polarizable case shown ($\mathcal{L}/c$ = 1), anodic and cathodic areas are the least affected by each other, there is the greatest drop in potential across the anode/cathode juncture, and hence there is some intensified attack at that boundary.

Figure 8 shows the effect of changing the cell dimensions. For a fixed anode radius and polarization parameter, an increase in cathode radius $c$ leads to intensified attack at

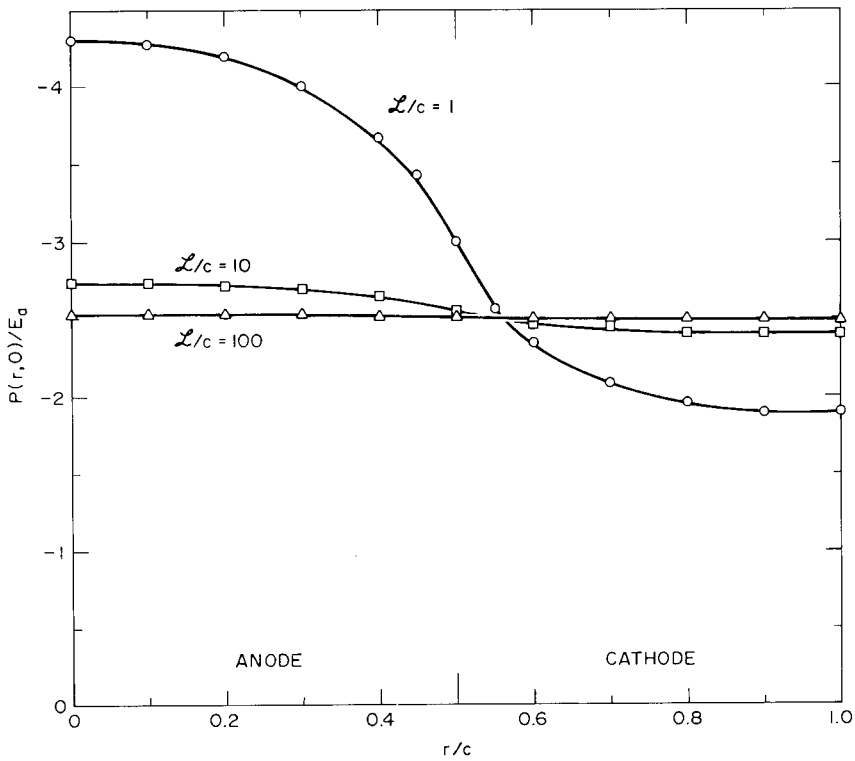


Fig. 6—Potential distribution under bulk electrolyte for different polarization parameters at a fixed cell size ($a/c$ = 0.5). ($E_c$ = 0.)

the anode/cathode boundary for the smaller $\mathfrak{L}$ only. There is no size effect for the more polarizable electrodes.

## THIN-LAYER ELECTROLYTE

### Summary of Equations

The case of a thin-layer electrolyte has been treated by Gal-Or and coworkers [8]. The boundary conditions are the same as the bulk case, except that the requirement that the potential be finite at the electrolyte/air interface,*

$$\lim_{z \to \infty} P(r, z) < M , \tag{16}$$

*or that there be no current across that interface.

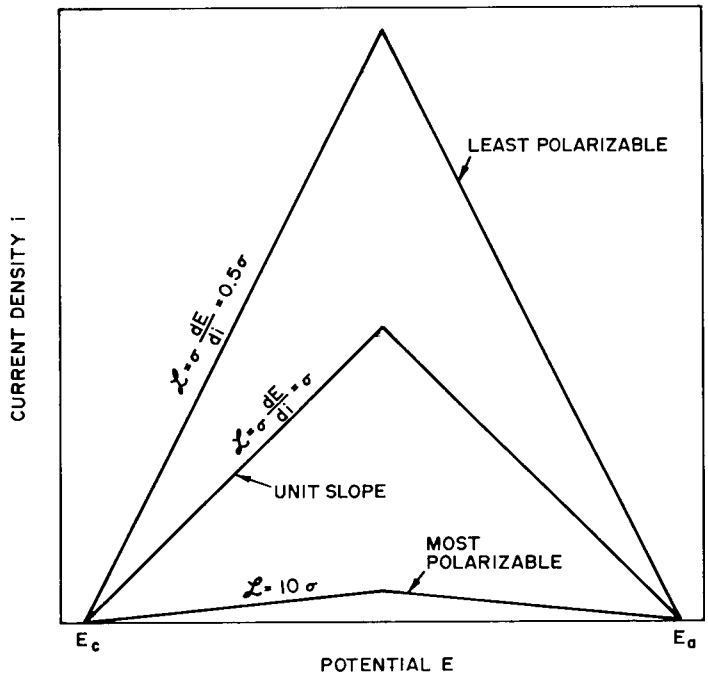


Fig. 7—Effect of the parameter $\mathfrak{L}$ on the polarization curve (schematic)

is replaced by the requirement that there be no current flow across the outer boundary $z = b$:

$$\left[\frac{\partial P(r,z)}{\partial z}\right]_{z=b} = 0 . \tag{24}$$

The solution to Laplace's equation subject to Eqs. (14), (15), (17) and (24) is:

$$P(r,z) = \left(\frac{a}{c}\right)^2 E_a + \left(\frac{c^2 - a^2}{c^2}\right) E_c$$

$$+ (E_a - E_c) \sum_{n=1}^{\infty} \frac{\frac{2}{x_n}\frac{a}{c} J_1\left(x_n \frac{a}{c}\right)}{\left[1 + \frac{\mathfrak{L}}{c} x_n \tanh\left(x_n \frac{b}{c}\right)\right]\left[J_0(x_n)\right]^2} e^{-x_n z/c} J_0\left(x_n \frac{r}{c}\right), \tag{25}$$

so that

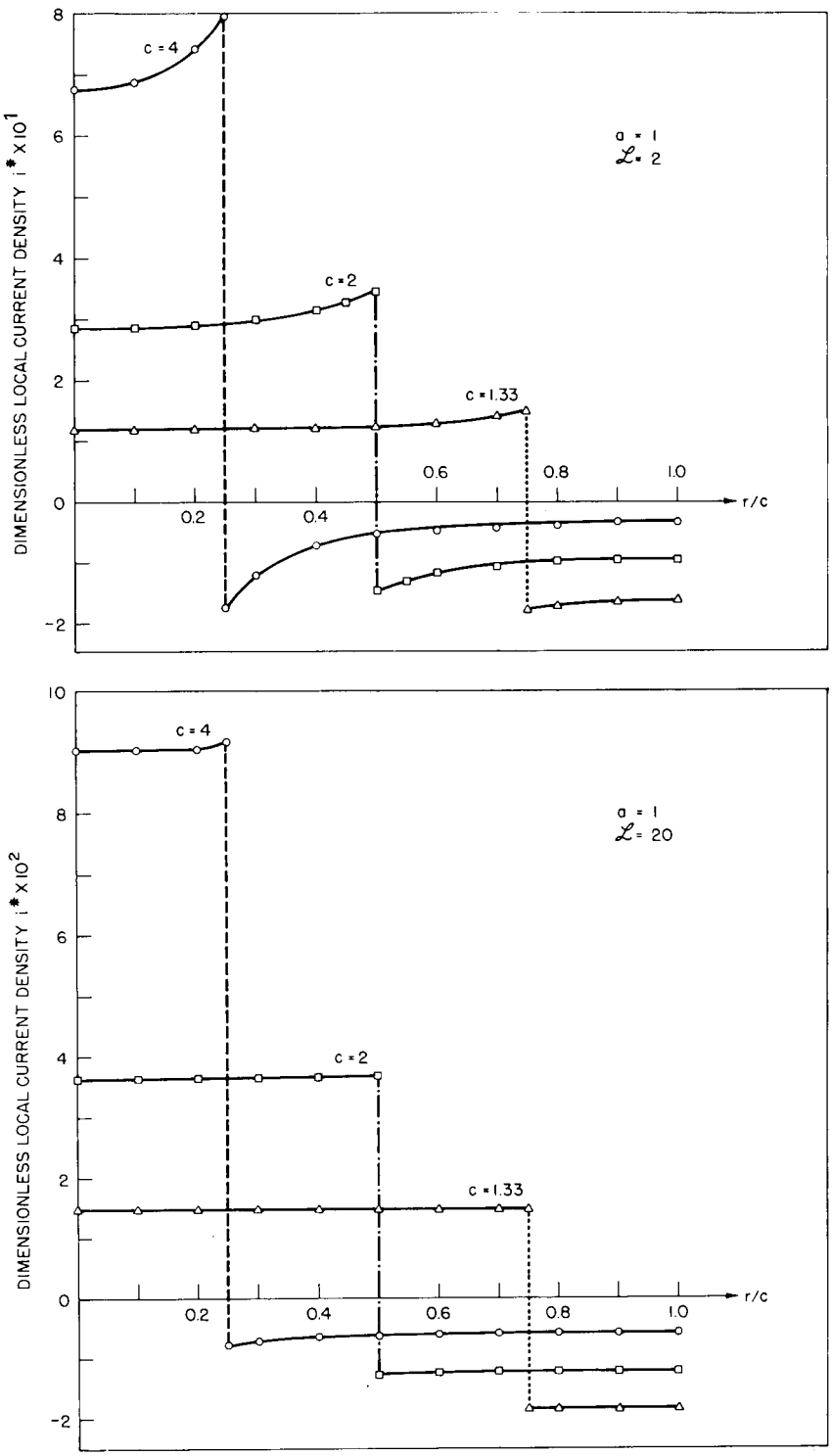


Fig. 8—Effect of a change in cathode size on the current distribution under bulk electrolyte for a fixed anode size and fixed polarization parameter

$$P(r, 0) = \left(\frac{a}{c}\right)^2 E_a + \left(\frac{c^2 - a^2}{c^2}\right) E_c$$

$$+ (E_a - E_c) \sum_{n=1}^{\infty} \frac{\frac{2}{x_n} \frac{a}{c} J_1\left(x_n \frac{a}{c}\right)}{\left[1 + \frac{\mathfrak{L}}{c} x_n \tanh\left(x_n \frac{b}{c}\right)\right] \left[J_0(x_n)\right]^2} J_0\left(x_n \frac{r}{c}\right) \qquad (26)$$

and‡

$$i^* \equiv \frac{i(r, 0)}{2\frac{\sigma}{c}(E_a - E_c)} = \sum_{n=1}^{\infty} \frac{\frac{a}{c} J_1\left(x_n \frac{a}{c}\right)}{\left[\coth\left(x_n \frac{b}{c}\right) + \frac{\mathfrak{L}}{c} x_n\right] \left[J_0(x_n)\right]^2} J_0\left(x_n \frac{r}{c}\right) . \qquad (27)$$

Again $i^*$ is dimensionless and may be termed the dimensionless local current density. It depends only on the cell dimensions $a/c$, $b/c$, $r/c$ and on the reduced polarization parameter $\mathfrak{L}/c$.

Both the hyperbolic tangent and hyperbolic cotangent approach unity as the argument becomes infinite, so that when the thickness $b$ of the electrolyte layer approaches infinity, Eqs. (26) and (27) in $P(r, 0)$ and $i^*$ respectively revert back to the expressions for the bulk electrolyte, that is, Eqs. (20) and (21).

## Numerical Evaluation

Evaluation of $i^*$ according to Eq. (29) is shown in Fig. 9 for different electrolyte thicknesses for a fixed cell size $a/c$ and a fixed reduced polarization parameter $\mathfrak{L}/c$. It is seen that the anodic current density is concentrated at the anode/cathode boundary for the thinner electrolyte layers. The corresponding potential distribution, calculated according to Eq. (26), is given in Fig. 10 (with $E_c$ again taken to be zero). Like the current distribution, the potential distribution is uniform only for the thicker electrolyte layers.

The effect of variable $\mathfrak{L}/c$ on $i^*$ for a fixed geometry (constant $a/c$ and $b/c$) is shown in Fig. 11. The smaller values of $\mathfrak{L}/c$ (less polarizable electrodes) lead to pronounced local attack near the edge of the anode. The corresponding potential distributions are shown in Fig. 12. As might be expected, the smaller values of $\mathfrak{L}/c$ produce the sharpest drops in potential at the anode/cathode juncture.

The effect of variable cell size on $i^*$ is shown in Fig. 13, where $a$, $b$, and $\mathfrak{L}$ are fixed but $c$ is allowed to vary. A decrease in the ratio of $a$ to $c$ leads to an increased local attack near the anode edge.

‡The expression by Gal-Or and coworkers for the local current density [Eq. (38) in Ref. 8] contains a misprint. Also, our notation follows Waber, so that $b$ and $c$ are interchanged relative to Ref. 8 and $\mathfrak{L}$ and $x_n$ replace $k$ and $k_n$ in Ref. 8.

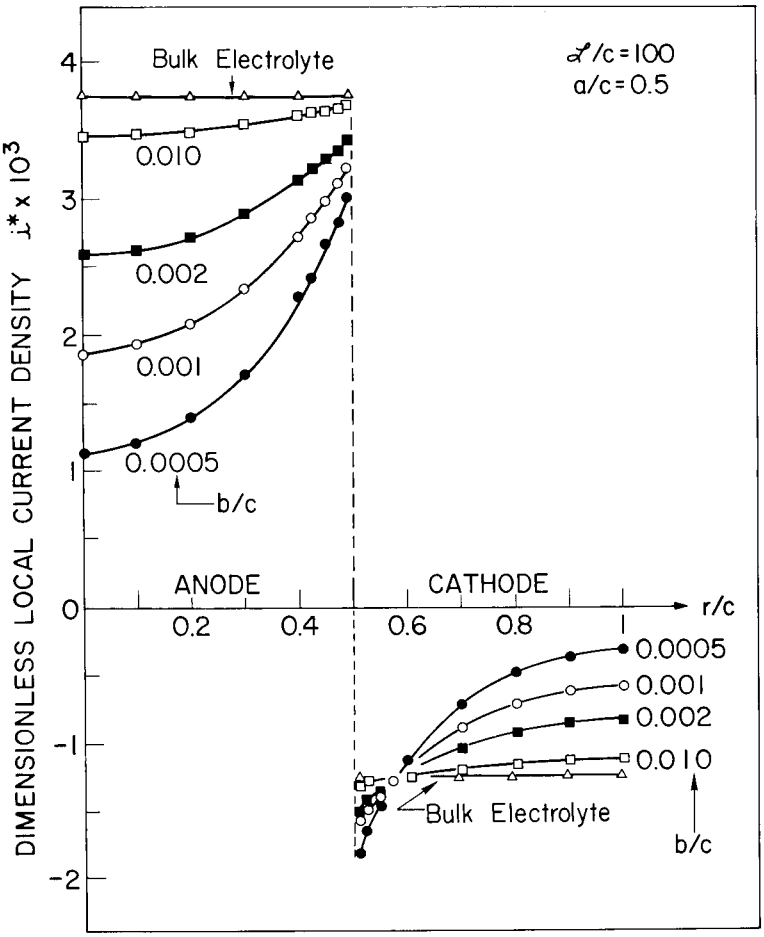


Fig. 9—Effect of electrolyte thickness on the current distribution for a fixed ratio of anode radius to cathode radius ($a/c$ = 0.5) and fixed polarization parameter ($\mathfrak{L}/c$ = 100). ($n$ = 500 except at $r/c$ = 0 and near 0.5, where $n$ = 2000 to 4000.)

In summary, for a fixed anode radius, local attack in thin electrolytes is promoted by decreasing:

- The electrolyte thickness $b$
- the polarization parameter $\mathfrak{L}$

or by increasing:

- the cathode radius $c$.

## Comparison with Experiment

Few experiments have been done with circular electrodes. However, this current mathematical analysis is in general agreement with the investigations of Rosenfeld and Pavlutskaya [15, 22]. For a circular iron anode in contact with a copper disc cathode,

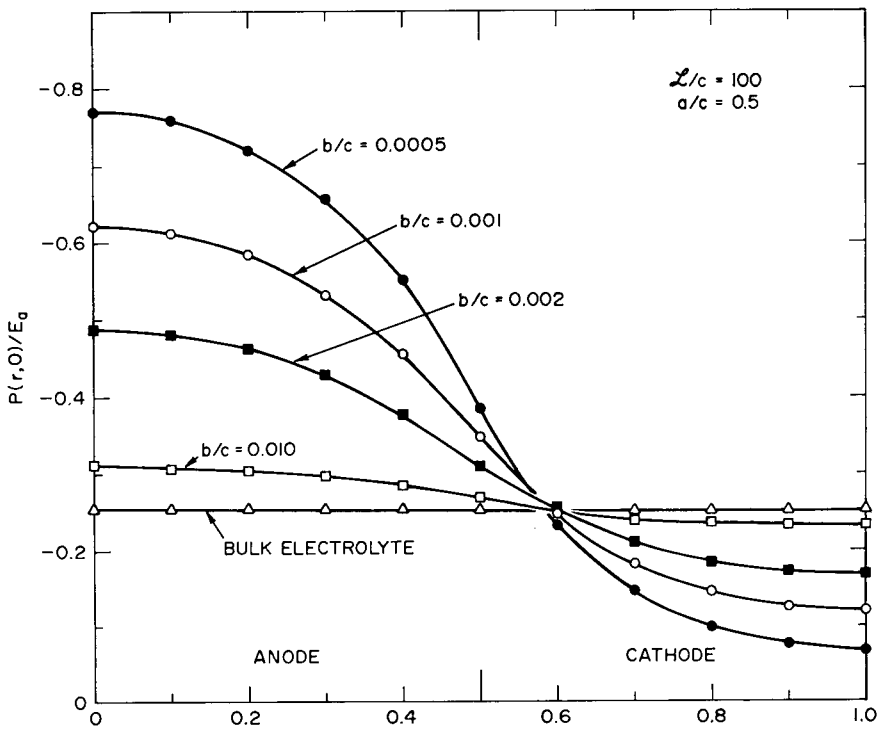


Fig. 10—Effect of electrolyte thickness on the potential distribution for a fixed ratio of anode radius to cathode radius ($a/c$ = 0.5) and fixed polarization parameter ($\mathfrak{L}/c$ = 100). ($E_c$ = 0, $n$ = 100.)

there was a non-uniform distribution of potential under a 165-$\mu$m layer of 0.1$N$ NaCl. The difference in potential between the points $r$ = 0 and $r$ = $c$ was nearly 300 m$V$, with most of the potential drop at the anode/cathode boundary. With bulk electrolyte, the potential distribution was more uniform with a potential drop of only 50 m$V$. Photomicrographs of the anode/cathode boundary profile showed that penetration near the contact was much greater with the thinner electrolyte.

These authors also reported current-distribution curves for a Cu/Zn couple which were conjoining rectangles rather than concentric circles. However, for that related geometry, the anodic attack was greatest near the anode edge for the thinnest electrolytes and was uniformly distributed for the bulk electrolyte (0.1$N$ NaCl).

In the case of another related geometry, where iron under crevices (thin electrolytes) was in contact with either iron or platinum under bulk electrolyte, the attack was intensified near the outermost edge of the iron anode [14].

## TOTAL CELL CURRENT

As mentioned earlier, Gal-Or, Raz, and Yahalom [8] have evaluated the total cell current rather than point-by-point values along the cell radius. These investigators showed that the total current increases with:

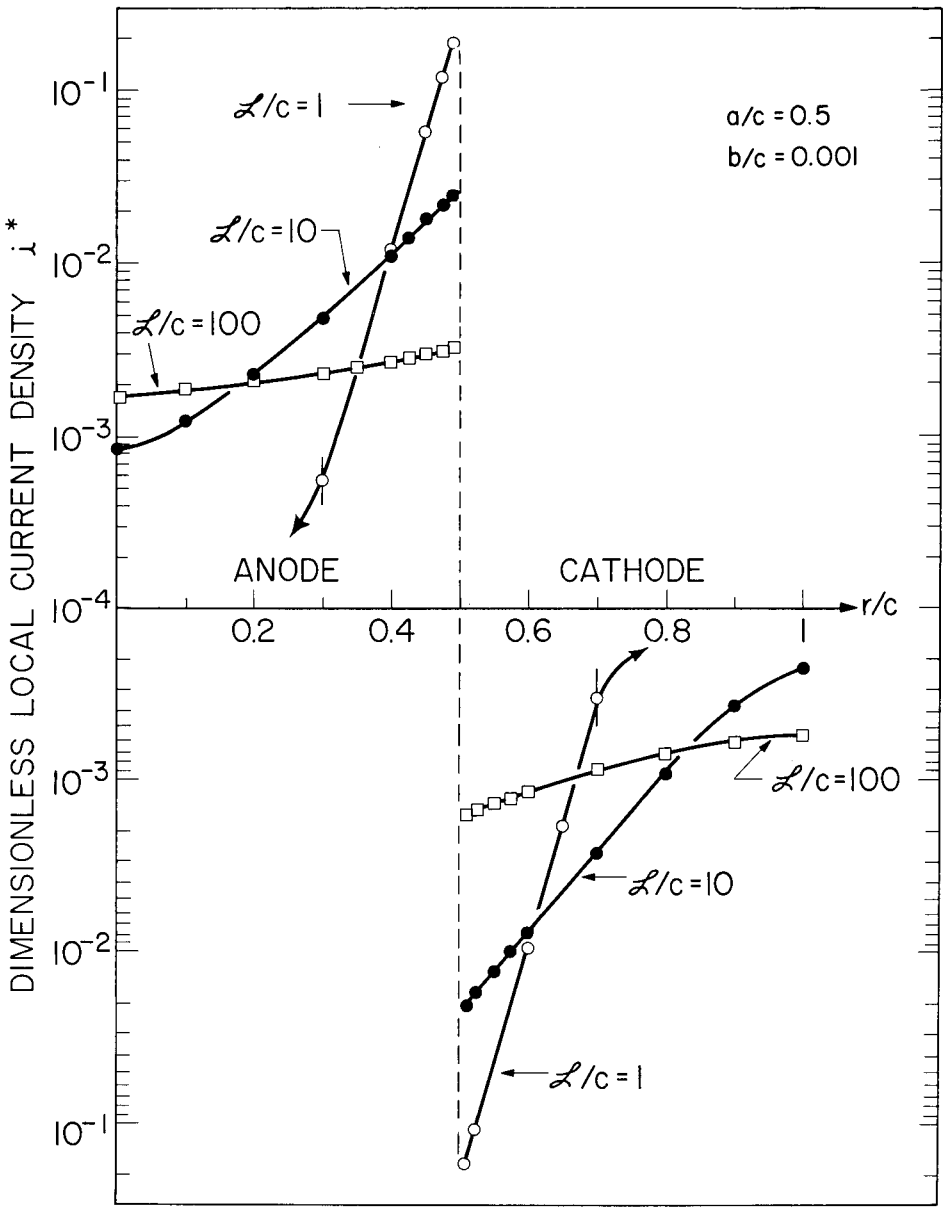


Fig. 11—Effect of polarization parameter on the current distribution for a fixed cell geometry ($a/c$ = 0.5, $b/c$ = 0.001). ($n$ = 2000 for $\mathfrak{L}/c$ = 1, $n$ = 1000 for $\mathfrak{L}/c$ = 10, and $n$ = 500 for $\mathfrak{L}/c$ = 100; in all cases, $n$ = 2000 to 4000 at 0 and near $a/c$.)

- increases in electrolyte thickness (up to a limit);
- decreases in polarization parameter;
- increases in anode radius (for a fixed cathode radius).

The total anodic current was evaluated by integrating the local current density:

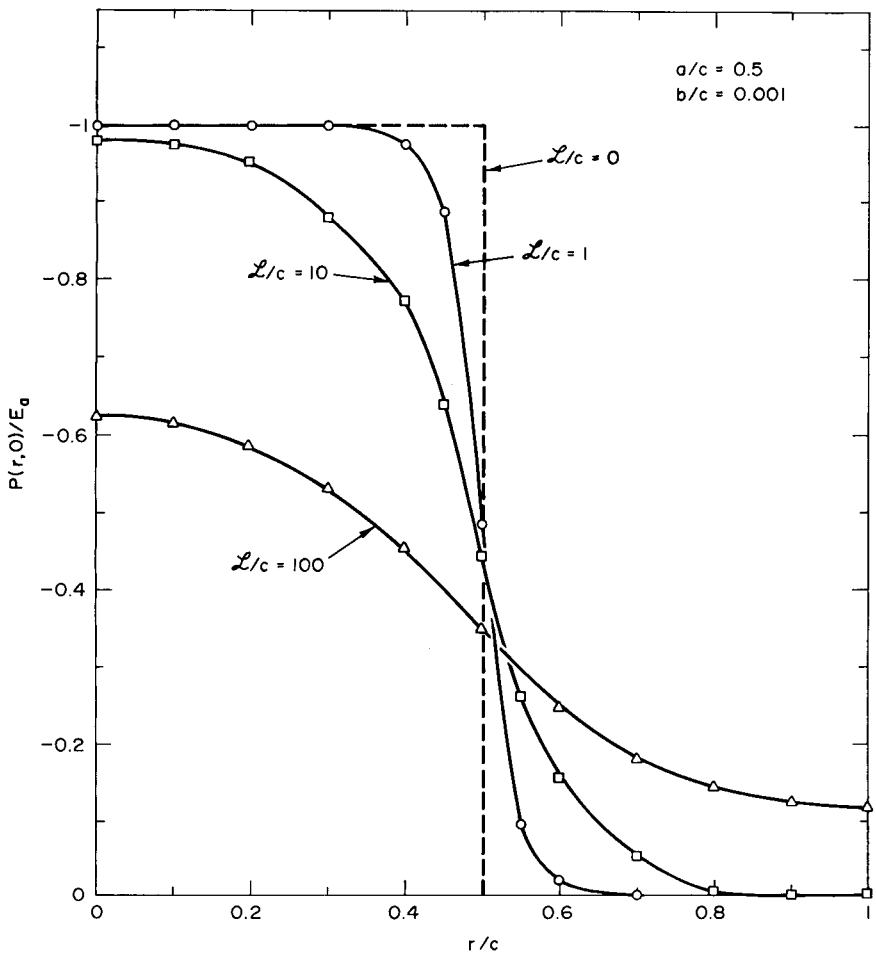


Fig. 12—Effect of polarization parameter on the potential distribution for a fixed cell geometry ($a/c$ = 0.5, $b/c$ = 0.001). ($E_c$ = 0, $n$ = 100.)

$$i_{\text{total,anodic}} = \int_{r=0}^{a} \int_{\theta=0}^{2\pi} i(r,\ 0)\ r\ dr d\theta \tag{28}$$

Use of $i(r,\ 0)$ from Eq. (27) for thin layers gives [8]

$$i_{\text{total,anodic}} = 4\pi\sigma c \left(\frac{a}{c}\right)^2 (E_a - E_c) \sum_{n=1}^{\infty} \frac{\left[J_1\left(x_n \frac{a}{c}\right)^2\right]}{\left[\coth\left(x_n \frac{b}{c}\right) + \frac{\varrho}{c} x_n\right] \left[J_0(x_n)\right]^2 x_n}. \tag{29}$$

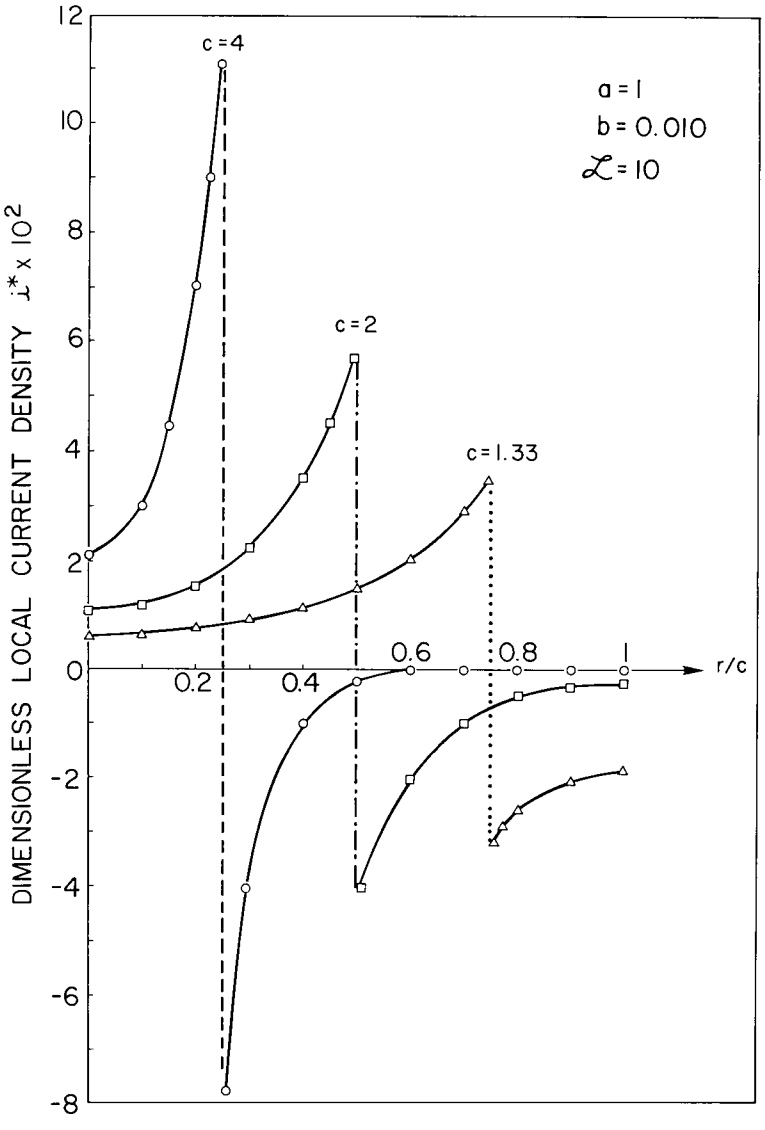


Fig. 13—Effect of cathode size on the current distribution (anode size, solution thickness, and polarization parameter are fixed)

For bulk electrolyte, the term coth $(x_n\ b/c)$ is replaced by 1. An internal check on the current distribution can be made by comparing the total current determined by mathematical integration from Eq. (29) with the total current determined by graphical integration of the current density distribution curve $[i^*(r/c)$ as a function of $r/c]$. By definition,

$$i^*(r, c) \equiv \frac{i(r, 0)}{2\,\frac{\sigma}{c}\,(E_a - E_c)}\,, \tag{23}$$

so that Eq. (28) can be written

$$i_{\text{total,anodic}} = 4\pi \frac{\sigma}{c} (E_a - E_c) \int_{r=0}^{r=a} i^*\left(\frac{r}{c}\right) r \, dr , \tag{30}$$

which can be put in the form

$$i_{\text{total,anodic}} = 4\pi\sigma c(E_a - E_c) \underbrace{\int_{r/c=0}^{r/c=a/c} i^*\left(\frac{r}{c}\right) \left(\frac{r}{c}\right) d\left(\frac{r}{c}\right)}_{G^*} . \tag{31}$$

The integral in Eq. (31), labeled $G^*$, can be determined graphically from current-distribution plots such as Figs. 5, 8, 9, 11 and 13. Comparison of Eqs. (29) and (31) shows that

$$\frac{i_{\text{total,anodic}}}{4\pi\sigma c(E_a - E_c)} = \left(\frac{a}{c}\right)^2 \Sigma = G^* , \tag{32}$$

where $\Sigma$ is the sum indicated in Eq. (29).

Table 3 shows that the total anodic current determined by graphical integration of the current density distribution curves is in agreement with values determined by mathematical integration after Gal-Or and coworkers. Table 3 also shows the effect of the various parameters on the total anodic current; these trends have already been reported by Gal-Or, Raz, and Yahalom [8] and are listed at the beginning of this section.

As a final check, the total cathodic current was computed in some cases by graphical integration of current density distribution curves from $r/c = a/c$ to $r/c = 1$. The total cathodic current was equal to the total anodic current, as required.

## SUMMARY

The distribution of current in a circular corrosion cell has been computed based on the assumption that the electrolyte has a uniform composition. The mathematical equations are summarized in Table 4. Numerical evaluation of the current-distribution function shows that:

- Current distribution is more uniform along the metal surface under bulk electrolytes than under thin layers of electrolyte.
- Under thin layers of electrolyte, corrosion attack is intensified at the anode/cathode junction. For a fixed anode radius, the local attack is promoted by:
  - a decrease in electrolyte thickness,
  - a decrease in the linear polarization parameter,
  - an increase in the cathode size,

where in each case the remaining parameters are held constant.

Table 3a
Comparison of the Total Anodic Current Determined by Mathematical and Graphical Integration for a Fixed Ratio of Anode Radius to Cathode Radius $a/c$

| $\frac{a}{c}$ | $\frac{\mathfrak{L}}{c}$ | $\frac{b}{c}$ | $10^3 \frac{i_{\text{total,anodic}}}{4\pi\sigma c(E_a - E_c)}$ | |
|---|---|---|---|---|
| | | | Mathematical Integration $\left(\frac{a}{c}\right)^2 \Sigma$ | Graphical Integration $G^*$ |
| 0.5 | 100 | 0.0005 | 0.252 | 0.250 |
| | | 0.001 | 0.318 | 0.317 |
| | | 0.002 | 0.375 | 0.379 |
| | | 0.01 | 0.445 | 0.445 |
| | | bulk | 0.467 | 0.468 |
| 0.5 | 10 | 0.001 | 1.23 | 1.17 |
| | 1 | | 3.92 | 3.71 |
| 0.5 | 100 | bulk | 0.467 | 0.468 |
| | 10 | | 4.59 | 4.56 |
| | 1 | | 38.8 | 38.1 |

Table 3b
Comparison of the Total Anodic Current Determined by Mathematical and Graphical Integration for Variable Cathode Size with $a = 1$, $b = 0.01$, $\mathfrak{L} = 10$

| $c$ | $\frac{a}{c}$ | $\frac{b}{c}$ | $\frac{\mathfrak{L}}{c}$ | $10^3 \frac{i_{\text{total,anodic}}}{4\pi\sigma(E_a - E_c)}$ | |
|---|---|---|---|---|---|
| | | | | Mathematical Integration $c\left(\frac{a}{c}\right)^2 \Sigma$ | Graphical Integration $cG^*$ |
| 4 | 0.25 | 0.0025 | 2.5 | 7.52 | 7.52 |
| 2 | 0.5 | 0.005 | 5 | 7.62 | 7.62 |
| 1.33 | 0.75 | 0.0075 | 7.5 | 6.67 | 6.66 |

Table 4
Summary of Equations for Circular Electrodes Under Thin Layers [8] and Bulk Electrolyte

| | |
|---|---|
| Potential at any point | $$P(r,z) = \left(\frac{a}{c}\right)^2 E_a + \left(\frac{c^2 - a^2}{c^2}\right) E_c + (E_a - E_c) \sum_{n=1}^{\infty} \frac{\frac{2}{x_n}\frac{a}{c} J_1\left(x_n \frac{a}{c}\right)}{\left(1 + \frac{\varrho}{c} x_n Q\right) \left[J_0(x_n)\right]^2} e^{-x_n z/c} J_0\left(x_n \frac{r}{c}\right).$$ |
| Potential along the metal surface | $$P(r,0) = \left(\frac{a}{c}\right)^2 E_a + \left(\frac{c^2 - a^2}{c^2}\right) E_c + (E_a - E_c) \sum_{n=1}^{\infty} \frac{\frac{2}{x_n}\frac{a}{c} J_1\left(x_n \frac{a}{c}\right)}{\left(1 + \frac{\varrho}{c} x_n Q\right) \left[J_0(x_n)\right]^2} J_0\left(x_n \frac{r}{c}\right),$$ <br> where $Q = \begin{cases} 1, & \text{bulk electrolyte;} \\ \tanh\left(x_n \frac{b}{c}\right), & \text{thin layers.} \end{cases}$ |
| Local current density | $$i^* = \frac{i(r,0)}{2\frac{\sigma}{c}(E_a - E_c)} = \sum_{n=1}^{\infty} \frac{\frac{a}{c} J_1\left(x_n \frac{a}{c}\right)}{\left[R + \frac{\varrho}{c} x_n\right] \left[J_0(x_n)\right]^2} J_0\left(x_n \frac{r}{c}\right),$$ <br> where $R = \begin{cases} 1, & \text{bulk electrolyte;} \\ \coth\left(x_n \frac{b}{c}\right), & \text{thin layers.} \end{cases}$ |

## REFERENCES


1. C. Wagner and W. Traud, *Z. Elektrochem.* **44**, 391 (1938).
2. J.T. Waber, *J. Electrochem. Soc.* **101**, 271 (1954).
3. J.T. Waber and M. Rosenbluth, *J. Electrochem. Soc.* **102**, 344 (1955).
4. J.T. Waber, *J. Electrochem. Soc.* **102**, 420 (1955).
5. J.T. Waber and B. Fagan, *J. Electrochem. Soc.* **103**, 64 (1956).
6. J.T. Waber, *J. Electrochem. Soc.* **103**, 567 (1956).
7. J.A. Simmons, S.R. Coriell, and F. Ogburn, *J. Electrochem. Soc.* **114**, 782 (1967).
8. L. Gal-Or, Y. Raz, and J. Yahalom, *J. Electrochem. Soc.* **120**, 598 (1973).
9. G. Herbsleb and H.J. Engell, *Z. Elektrochem.* **65**, 881 (1961).
10. A. Cohen and W.S. Lyman, *Materials Protection and Performance* **11**, No. 2, 48 (1972).
11. B.F. Brown, *Machine Design* **40**, No. 2, 165 (1968).
12. J. Newman, in "Advances in Electrochemistry and Electrochemical Engineering" (C. W. Tobias, editor), Vol. 5, Interscience, New York, 1967, p. 87.
13. C. Wagner, *J. Electrochem. Soc.* **98**, 116 (1951).
14. E. McCafferty, *J. Electrochem. Soc.* **121**, 1007 (1974).
15. I.L. Rozenfeld, "Atmospheric Corrosion of Metals," published by National Association of Corrosion Engineers, Houston, 1973, p. 60.
16. J.T. Waber, *Corrosion* **13**, 95t (1957).
17. M.H. Peterson, T.J. Lennox, Jr., and R.E. Groover, *Materials Protection* **9**, No. 1, 23 (1970).
18. T. Suzuki, M. Yamabe, and Y. Kitamura, *Corrosion* **29**, 18 (1973).
19. M. Pourbaix, in "The Theory of Stress Corrosion Cracking in Alloys" (J. C. Schully, editor), NATO, Brussels, 1971, p. 17.
20. C.T. Fujii, Belgian Center for Corrosion Study (CEBELCOR) Report RT 213, Jan. 1974.
21. A. Heydweiller, *Z. Anorg. u. allg. Chem.* **116**, 42 (1921).
22. I.L. Rosenfeld and T.I. Pavlutskaya, *Zh. Fiz. Khim.* **21**, 329 (1957).

## APPENDIX A

## MATHEMATICAL SOLUTION FOR THE ELECTRODE POTENTIAL OF CIRCULAR CELLS UNDER BULK ELECTROLYTE

In cylindrical coordinates, Laplace's equation

$$\frac{\partial^2 P(x, y, z)}{\partial x^2} + \frac{\partial^2 P(x, y, z)}{\partial y^2} + \frac{\partial^2 P(x, y, z)}{\partial z^2} = 0 \tag{A1}$$

becomes

$$\frac{\partial^2 P(r, z)}{\partial r^2} + \frac{1}{r}\frac{\partial P(r, z)}{\partial r} + \frac{\partial^2 P(r, z)}{\partial z^2} = 0\,, \tag{A2}$$

where the $\theta$ term is deleted because $P$ is not $\theta$ dependent. The general solution to Eq. (A2) is well known but will be outlined here for the convenience of the reader. One method of solution is separation of variables, in which solutions of the form

$$P(r, z) = R(r)Z(z) \tag{A3}$$

are sought. Thus

$$\frac{\partial P}{\partial r} = R'(r)Z(z)\,, \tag{A4a}$$

$$\frac{\partial^2 P}{\partial r^2} = R''(r)Z(z)\,, \tag{A4b}$$

and

$$\frac{\partial^2 P}{\partial z^2} = R(r)\ddot{Z}(z)\,, \tag{A4c}$$

where the prime and dot indicate differentiation with respect to $r$ and $z$ respectively. Using Eqs. (A4) in Eq. (A2) and making appropriate rearrangements gives

$$\frac{R''(r)}{R(r)} + \frac{1}{r}\frac{R'(r)}{R(r)} = -\frac{\ddot{Z}(z)}{Z(z)} \tag{A5}$$

The left side is now a function of $r$ only and the right side of $z$ only, so that each side of Eq. (A5) can be set equal to an arbitrary constant, $-\lambda^2$. That is,

$$\frac{R''(r)}{R(r)} + \frac{1}{r}\frac{R'(r)}{R(r)} = -\lambda^2, \tag{A6}$$

and

$$-\frac{\ddot{Z}(z)}{Z(z)} = -\lambda^2 . \tag{A7}$$

The first separated equation is thus

$$R''(r) + \frac{1}{r}R'(r) + \lambda^2 R(r) = 0 . \tag{A8}$$

After making the substitution $s = \lambda r$, which defines $s$, and performing some algebraic manipulations, Eq. (A8) takes the form

$$\frac{d^2R}{ds^2} + \frac{1}{s}\frac{dR}{ds} + \left(1 - \frac{p^2}{s^2}\right) R = 0 \qquad (p = 0), \tag{A9}$$

which is Bessel's equation of order $p$ and has the independent solutions [A1, A2] $R = J_p(s)$ and $R = Y_p(s)$, where $J_p(s)$ is the Bessel function* of the first kind of order $p$ and $Y_p(s)$ is Neumann's Bessel function† of the second kind of order $p$. The general solution to Eq. (A9) is then

$$R(r) = AJ_0(\lambda r) + BY_0(\lambda r) , \tag{A10}$$

where $A$ and $B$ are constants. The solution to the second separated equation

$$\ddot{Z}(z) - \lambda^2 Z(z) = 0 \tag{A11}$$

is

$$Z(z) = C_1' e^{\lambda z} + C_2' e^{-\lambda z} , \tag{A12}$$

---

*$J_p(s) = \left(\frac{s}{2}\right)^p \sum_{n=0}^{\infty} \frac{\left(\frac{s}{2}\right)^{2n} (-1)^n}{n!(p+n)!}$.

†$Y_0(s) = J_0(s) \log s + \frac{s^2}{2^2} - \frac{s^4}{2^2 \cdot 4^2}\left(1 + \frac{1}{2}\right) + \frac{s^6}{2^2 \cdot 4^2 \cdot 6^2}\left(1 + \frac{1}{2} + \frac{1}{3}\right) - \ldots$ .

where $C_1'$ and $C_2'$ are constants. Use of Eqs. (A10) and (A12) in Eq. (A3) gives the general solution of Laplace's equation:

$$P(r, z) = [AJ_0(\lambda r) + BY_0(\lambda r)] [C_1' e^{\lambda z} + C_2' e^{-\lambda z}] . \tag{A13}$$

The constants $A$, $B$, $C_1'$, and $C_2'$ are to be evaluated from the specific boundary conditions, which have been listed previously:

$$\left[\frac{\partial P(r, z)}{\partial r}\right]_{r=0} = 0 \tag{A14}$$

$$\left[\frac{\partial P(r, z)}{\partial r}\right]_{r=c} = 0 \tag{A15}$$

$$\lim_{z \to \infty} P(r, z) < M \tag{A16}$$

$$P(r, z) - \mathfrak{L}\left[\frac{\partial P(r, z)}{\partial z}\right]_{z=0} = \begin{cases} E_a, & 0 \leqslant r < a ; \\ E_c, & a < r \leqslant c . \end{cases} \tag{A17}$$

Differentiation of Eq. (A13) gives

$$\frac{\partial P(r, z)}{\partial r} = [-A\lambda J_1(\lambda r) - B\lambda Y_1(\lambda r)] [C_1' e^{\lambda z} + C_2' e^{-\lambda z}] . \tag{A18}$$

According to the boundary condition of Eq. (A14), $P_r(r, z) = 0$ when $r = 0$, so that

$$-A\lambda J_1(0) - B\lambda Y_1(0) = 0 , \tag{A19}$$

which requires that $B = 0$ because $Y_1(0)$ is infinite and $J_1(0)$ is already zero [A2]. If we write $AC_1' = C_1$, and $AC_2' = C_2$, then

$$P(r, z) = J_0(\lambda r) [C_1 e^{\lambda z} + C_2 e^{-\lambda z}] . \tag{A20}$$

According to the boundary condition of Eq. (A15), $P_r(r, z) = 0$ at $r = c$, so that

$$-\lambda J_1(\lambda c) [C_1 e^{\lambda z} + C_2 e^{-\lambda z}] = 0 , \tag{A21}$$

or

$$J_1(\lambda c) = 0 . \tag{A22}$$

Let these roots of $J_1$ which give $J_1(x) = 0$ be called $x_n$, as shown in Fig. A1; that is,

$$x_n = \lambda_n c , \qquad n = 1, 2, 3, \ldots , \tag{A23}$$

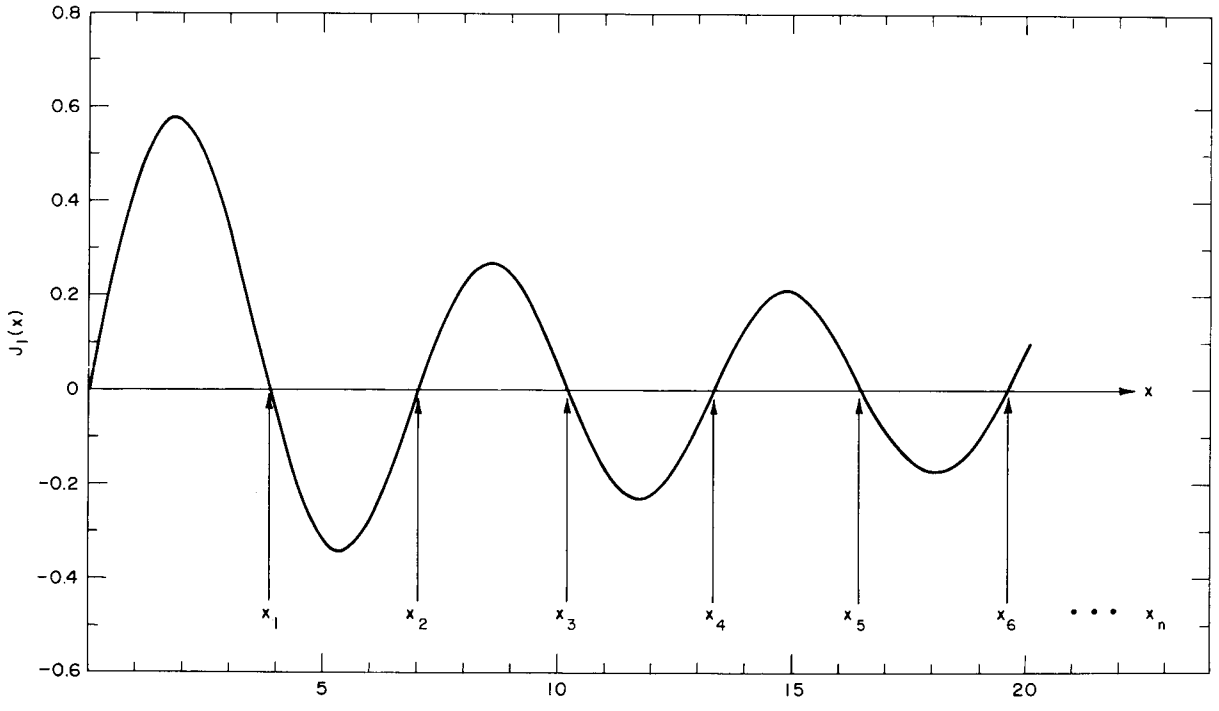


Fig. A1—Zeros of the Bessel function $J_1(x)$, denoted by $x_n$

or

$$\lambda_n = \frac{x_n}{c} . \tag{A24}$$

Thus

$$P(r, z) = J_0\left(x_n \frac{r}{c}\right) \left[C_1 e^{x_n z/c} + C_2 e^{-x_n z/c}\right] . \tag{A25}$$

The boundary condition of Eq. (A16), which requires $P(r, z)$ to be bounded, is satisfied if $C_1 = 0$. Thus

$$P(r, z) = C_2 J_0\left(x_n \frac{r}{c}\right) e^{-x_n z/c} \tag{A26}$$

is a particular solution to the problem. The general solution is then a linear combination of all the $n$ solutions:

$$P(r, z) = C_0 + \sum_{n=1}^{\infty} C_n J_0(\lambda_n r) e^{-\lambda_n z}, \tag{A27}$$

with $\lambda_n = x_n/c$. The constants $C_n$ are evaluated from the remaining boundary condition:

$$P(r, 0) - \mathfrak{L}\left[\frac{\partial P(r, z)}{\partial z}\right]_{z=0} = S(r) = \begin{cases} E_a, & 0 \leqslant r < a ; \\ E_c, & a < r \leqslant c . \end{cases} \tag{A17}$$

From Eq. (A27),

$$P(r, 0) = C_0 + \sum_{n=1}^{\infty} C_n J_0(\lambda_n r) , \tag{A28}$$

and

$$- \mathfrak{L}\left[\frac{\partial P(r, z)}{\partial z}\right]_{z=0} = \mathfrak{L} \sum_{n=1}^{\infty} C_n \lambda_n J_0(\lambda_n r) . \tag{A29}$$

Using Eqs. (A28) and (A29) in Eq. (A17) gives

$$C_0 + \sum_{n=1}^{\infty} C_n J_0(\lambda_n r) + \sum_{n=1}^{\infty} \mathfrak{L} \lambda_n C_n J_0(\lambda_n r) = S(r) , \tag{A30}$$

or

$$C_0 + \sum_{n=1}^{\infty} C_n (1 + \mathfrak{L} \lambda_n) J_0(\lambda_n r) = S(r) . \tag{A31}$$

One next employs the orthogonal property [A3]:

$$\int_{r=0}^{c} r J_0(\lambda_n r) J_0(\lambda_m r)\, dr = \begin{cases} 0, & n \neq m ; \\ \dfrac{c^2}{2} [J_0(\lambda_m c)]^2, & n = m . \end{cases} \tag{A32}$$

Multiplying both sides of Eq. (A31) by $r J_0(\lambda_m r)\, dr$ and integrating from $r = 0$ to $r = c$ gives the left-hand side (L.H.S.) of the equation to be

$$\text{L.H.S.} = \int_{r=0}^{c} C_0 r J_0(\lambda_m r)\, dr + \int_{r=0}^{c} \sum_{n=1}^{\infty} C_n (1 + \mathfrak{L} \lambda_n) r J_0(\lambda_n r) J_0(\lambda_m r)\, dr \tag{A33}$$

and the right-hand side (R.H.S.) to be

$$\text{R.H.S.} = \int_{r=0}^{c} S(r) r J_0(\lambda_m r)\, dr\,. \tag{A34}$$

The first integral in Eq. (A33), denoted as $I_1$:

$$I_1 \equiv \int_{r=0}^{c} C_0 r J_0(\lambda_m r)\, dr\,, \tag{A35}$$

is evaluated first. It can be shown [A2] that

$$\int r J_0(\lambda_m r)\, dr = \frac{1}{\lambda_m} [r J_1(\lambda_m r)]\,, \tag{A36}$$

so that

$$I_1 = \frac{C_0}{\lambda_m} [c J_1(\lambda_m c)]\,, \tag{A37}$$

but $J_1(\lambda_m c) = 0$ according to Eq. (A22). Thus $I_1 = 0$, so that

$$\text{L.H.S.} = \sum_{n=1}^{\infty} \left[ C_n (1 + \mathfrak{L}\lambda_n) \int_0^c r J_0(\lambda_n r) J_0(\lambda_m r)\, dr \right]\,. \tag{A38}$$

All terms are zero for $n \neq m$, so the only term which survives the integration is

$$\text{L.H.S.} = C_m (1 + \mathfrak{L}\lambda_m) \frac{c^2}{2} [J_0(\lambda_m c)]^2. \tag{A39}$$

Operating on the right-hand side,

$$\text{R.H.S.} = \int_{r=0}^{a} S(r) r J_0(\lambda_m r)\, dr + \int_{r=a}^{c} S(r) r J_0(\lambda_m r)\, dr\,, \tag{A40}$$

or

$$\text{R.H.S.} = E_a \int_{r=0}^{a} r J_0(\lambda_m r)\, dr + E_c \int_{r=a}^{c} r J_0(\lambda_m r)\, dr\,. \tag{A41}$$

Use of Eq. (A36) gives

$$\text{R.H.S.} = \frac{E_a}{\lambda_m} [a J_1(\lambda_m a)] + \frac{E_c}{\lambda_m} [c J_1(\lambda_m c) - a J_1(\lambda_m a)]\,, \tag{A42}$$

but again $J_1(\lambda_m c) = 0$; thus

$$\text{R.H.S.} = \frac{a}{\lambda_m} J_1(\lambda_m a)\,(E_a - E_c)\,. \tag{A43}$$

Equating Eqs. (A39) and (A43) gives

$$C_m(1 + \mathfrak{L}\lambda_m)\frac{c^2}{2}\,[J_0(\lambda_m c)]^2 = \frac{a}{\lambda_m} J_1(\lambda_m a)\,(E_a - E_c)\,. \tag{A44}$$

Solving for $C_m$ and replacing the dummy variable $m$ by $n$ gives the coefficients $C_n$:

$$C_n = \frac{\frac{a}{\lambda_n} J_1(\lambda_n a)\,(E_a - E_c)}{(1 + \mathfrak{L}\lambda_n)\frac{c^2}{2}\,[J_0(\lambda_n c)]^2}\,. \tag{A45}$$

One next solves for $C_0$. This time each side of Eq. (A31) is multiplied by $r\,dr$ and integrated from $r = 0$ to $r = c$:

$$C_0 \int_{r=0}^{c} r\,dr + \int_{r=0}^{c} \sum_{n=1}^{\infty} C_n(1 + \mathfrak{L}\lambda_n) r J_0(\lambda_n r)\,dr = \int_{r=0}^{c} S(r)\,dr\,. \tag{A46}$$

Here the second term vanishes, as may be seen by evaluating the integral according to Eq. (A36). Again the right-hand side of Eq. (A46) must be split into two integrals. The result of the simple integrations in Eq. (A46) is

$$C_0 = \left(\frac{a}{c}\right)^2 E_a + \left(\frac{c^2 - a^2}{c^2}\right) E_c \tag{A47}$$

Use of the expressions for $C_n$ and $C_0$, as given by Eqs. (A45) and (A47), in Eq. (A27) with $\lambda_n = x_n/c$ gives the desired expression for the potential distribution in the system:

$$P(r,z) = \left(\frac{a}{c}\right)^2 E_a + \left(\frac{c^2 - a^2}{c^2}\right) E_c + (E_a - E_c) \sum_{n=1}^{\infty} \frac{\frac{2}{x_n}\frac{a}{c} J_1\left(x_n \frac{a}{c}\right)}{\left(1 + \frac{\mathfrak{L}}{c} x_n\right)\,[J_0(x_n)]^2} e^{-x_n z/c} J_0\left(x_n \frac{r}{c}\right)\,. \tag{A48}$$

## REFERENCES


A1. A. Gray and G.B. Mathews, "A Theatise on Bessel Functions and Their Applications to Physics," 2nd ed., Chapter I, McMillan, London, 1922.

A2. F.E. Relton, "Applied Bessel Functions," Chapters IV and VI, Dover, New York, 1965.

A3. H.F. Davis, "Fourier Series and Orthogonal Functions," Allyn and Bacon, Boston, 1963, p. 240.

# APPENDIX B
# COMPUTER PROGRAM FOR EVALUATION OF LOCAL CURRENT DENSITY FOR COPLANAR CONCENTRIC CIRCULAR ELECTRODES UNDER BULK ELECTROLYTE

```
**********************************************************************

      PROGRAM BULK1
C
C     THIS PROGRAM COMPUTES THE LOCAL CURRENT DENSITY ALONG THE RADIUS
C     FOR CO-PLANAR CIRCULAR ELECTRODES COVERED BY BULK ELECTROLYTE
C     FOR THE CASE WHERE ANODIC AND CATHODIC WAGNER POLARIZATION
C     PARAMETERS ARE EQUAL.
C
C     A=RADIUS OF ANODE
C     C=RADIUS OF CATHODE
C     R=DISTANCE ALONG RADIUS
C     L=WAGNER POLARIZATION PARAMETER
C     A/C=AR
C     L/C=LR
C     R/C=RR
C     X(N)=NTH ZERO OF BESSEL FUNCTION OF ORDER JORD
C
      REAL LR,NUM2
      DIMENSION X(5000),FACTOR(5000),TERM(5000)
      K=500
C     K=NUMBER OF TERMS IN SUM
      READ 10,AR,LR
   10 FORMAT (2F10.0)
      PRINT 11,AR,LR
   11 FORMAT (1H1,5X,7HAR=A/C= F10.5,5X,7HLR=L/C= F10.5,///)
      PRINT 101
  101 FORMAT (25X,*J (X(N))*,5X,8HX(N)*A/C,7X,*J (P)*,4X,11H(A/C)*J (P))
      PRINT 102
  102 FORMAT (26X,*0*,27X,*1*,14X,*1*,/)
      PRINT 103
  103 FORMAT (6X,*N*,6X,*X(N)*,9X,*BESSEL2*,9X,*P*,9X,*BESSEL1*,8X,
     **NUM2*,8X,*DENOM1*,8X,*DENOM2*,7X,*FACTOR(N)*,///)
      JORD=1
      NO=K
      CALL BESZERO(JORD,NO,X)
      DO 20 N=1,K
      P=X(N)*AR
      T=X(N)*LR
      BESSEL1=BESJ(P,1)
      NUM2=AR*BESSEL1
      DENOM1=1.0 + T
      BESSEL2=BESJ(X(N),0)
      DENOM2=BESSEL2**2
      FACTOR(N)=NUM2/(DENOM1*DENOM2)
      PRINT 19,N,X(N),BESSEL2,P,BESSEL1,NUM2,DENOM1,DENOM2,FACTOR(N)
   19 FORMAT (3X,I4,4(3X,F10.5),4(1X,E13.5))
   20 CONTINUE
      READ 201,RR,DELTA,RCUT
  201 FORMAT (F10.0)
   21 PRINT 22,RR
   22 FORMAT (///3X,*RR= *F5.3///)
      PRINT 221
```

```
  221 FORMAT (25X,8HX(N)*R/C,7X,*J (W)*)
      PRINT 222
  222 FORMAT (41X,*0*,/)
      PRINT 223
  223 FORMAT (6X,*N*,7X,*X(N)*,11X,*W*,9X,*BESSEL3*,6X,*FACTOR(N)*,8X,
     **TERM(N)*,11X,*SUM*,///)
      SUM=0.0
      DO 30 N=1,K
      W=X(N)*RR
      BESSEL3=BESJ(W,0)
      TERM(N)=FACTOR(N)*BESSEL3
      SUM=SUM+TERM(N)
      PRINT 29,N,X(N),W,BESSEL3,FACTOR(N),TERM(N),SUM
   29 FORMAT (3X,I4,1X,E12.5,2(3X,F10.5),3(3X,E15.5))
   30 CONTINUE
      RR=RR+DELTA
      IF (RR.LE.RCUT) GO TO 21
   99 END
C
      SUBROUTINE BESZERO(JORD,NO,ZERO)                                    00000100
C     IDENT NUMBER - C3007R00                                             00000101
C     TITLE - ZEROS OF THE BESSEL FUNCTION OF THE FIRST KIND              00000102
C     IDENT NAME - C3-NRL-BESZERO                                         00000103
C     LANGUAGE - 3600/380  FORTRAN                                        00000104
C     COMPUTER - CDC-3800                                                 00000105
C     CONTRIBUTOR - JANET P. MASON, CODE 7813                             00000106
C                   RESEARCH COMPUTATION CENTER, MIS DIVISION             00000107
C     ORGANIZATION - NRL - NAVAL RESEARCH LABORATORY,                     00000108
C                    WASHINGTON, D.C. 20390                               00000109
C     DATE - 1 JULY 1971                                                  00000110
C     PURPOSE - TO FIND THE FIRST M ZEROS OF JSUBN(X) FOR 0≤N≤5, WHERE    00000111
C               M IS SUPPLIED, BY THE USER, IN THE SUBROUTINE CALL        00000112
      DIMENSION XJA0(4),XJA1(3),XJA2(2),XJA3(6),XJA4(6),XJA5(9),ZERO(1)   00000200
      DATA(XJA0=2.4048255577,5.5200781103,8.6537279129,11.791534439),     00000300
     1     (XJA1=3.8317059702,7.0155866698,10.173468135),                 00000400
     2     (XJA2=5.1356223,8.4172441),                                    00000500
     3     (XJA3=6.3801619,9.7610231,13.0152007,16.2234640,19.4094148,    00000600
     4           22.5827295),                                             00000700
     5     (XJA4=7.5883427,11.0647095,14.3725367,17.6159660,20.8269330,   00000800
     6           24.0190195),                                             00000900
     7     (XJA5=8.7714838,12.3386042,15.7001741,18.9801339,22.2177999,   00001000
     8           25.4303411,28.6266183,31.8117167,34.9887813)             00001100
      PI=3.1415926536                                                     00001200
      HOLD=4.0*JORD*JORD                                                  00001300
      GO TO (1,2,3,4,5,6),JORD+1                                          00001400
    1 DO 11 I=1,NO                                                        00001500
      IF(I.GT.4)GO TO 20                                                  00001600
      ZERO(I)=XJA0(I)                                                     00001700
   11 CONTINUE                                                            00001800
      RETURN                                                              00001900
    2 DO 12 I=1,NO                                                        00002000
      IF(I.GT.3)GO TO 20                                                  00002100
      ZERO(I)=XJA1(I)                                                     00002200
   12 CONTINUE                                                            00002300
      RETURN                                                              00002400
    3 DO 13 I=1,NO                                                        00002500
      IF(I.GT.2)GO TO 20                                                  00002600
      ZERO(I)=XJA2(I)                                                     00002700
   13 CONTINUE                                                            00002800
      RETURN                                                              00002900
    4 DO 14 I=1,NO                                                        00003000
      IF(I.GT.6)GO TO 20                                                  00003100
      ZERO(I)=XJA3(I)                                                     00003200
   14 CONTINUE                                                            00003300
      RETURN                                                              00003400
```

```
    5 DO 15 I=1,NO                                                          00003500
      IF(I.GT.6)GO TO 20                                                    00003600
      ZERO(I)=XJA4(I)                                                       00003700
   15 CONTINUE                                                              00003800
      RETURN                                                                00003900
    6 DO 16 I=1,NO                                                          00004000
      IF(I.GT.9)GO TO 20                                                    00004100
      ZERO(I)=XJA5(I)                                                       00004200
   16 CONTINUE                                                              00004300
      RETURN                                                                00004400
   20 BETA=(PI/4.0)*(2.0*JORD+4.0*I-1.0)                                    00004500
      W1=BETA*8.0                                                           00004600
      W2=W1*W1                                                              00004700
      ZERO(I)=BETA-(HOLD+1.0)/W1*(1.0+1.0/W2*(4.0*(7.0*HOLD-31.0)/3.0       00004800
     1      +1.0/W2*(32.0*(83.0*HOLD*HOLD-982.0*HOLD+3779.0)/15.0           00004900
     2      +1.0/W2*(64.0*(6949.0*HOLD*HOLD*HOLD-153855.0*HOLD*HOLD         00005000
     3      +1585743.0*HOLD-6277237.0)/105.0))))                           00005100
      GO TO (11,12,13,14,15,16)JORD+1                                       00005200
   10 END                                                                   00005300
C
      FUNCTION BESJ(X,N)                                                    BESJ   1
      DATA(R0=.2827844947E8),(R1=-.685265989 1E7),(R2=.38831312263E6),      BESJ   2
     1(R3=-.90578674277E4),(R4=.108306963E3),(R5=-.73 85335935),            BESJ   3
     2(R6=.29212672487E-2),(R7=-.65050170571E-5),(R8=.64538018051E-8),      BESJ   4
     3(S0=.2827844947E8),(S1=.21695247743E6),(S2=.70046825147E3),           BESJ   5
     4(A0=2.5323420902E2),(A1=4.2217704118E1),(A2=5.2443314672E-1),         BESJ   6
     5(B0=.44884594896E3),(B1=.75322048579E2),                              BESJ   7
     6(C0=-1.2339445551E1),(C1=-2.7788921059),(C2=-4.9517399126E-2),        BESJ   8
     7(D1=.4100554523E2),(E=64.),(G=4.7223664 8E21),                        BESJ   9
     8(D0=.17496878239E3),                                                  BESJ  10
     A(RR0=.98087274959E7),(RR1=-.11425325721E7),(RR2=.40946213625E5),      BESJ  11
     B(RR3=-.66660119856E3),(RR4=.57575414035E1),(RR5=-.27904475519E-1),    BESJ  12
     C(RR6=.73493132111E-4),(RR7=-.84306821641E-7),                         BESJ  13
     D(SS0=.19617454991E8),(SS1=.16711673184E6),(SS2=.60777258247E3),       BESJ  14
     E(BB0=.62836856631E3),(BB1=.97300094628E2),                            BESJ  15
     F(DD0=.21185478331E3),(DD1=.46917127629E2),                            BESJ  16
     G(AA0=3.5451899975E2),(AA1=5.5544843021E1),(AA2=6.5223084285E-1),      BESJ  17
     H(CC0=4.4822348228E1),(CC1=9.7348068764),(CC2=1.7725579145E-1)         BESJ  18
      D=X*X                                                                 BESJ  19
      IF(N.EQ.0) GO TO 6 $ IF(N.EQ.1) GO TO 7 $ GO TO 8                     BESJ  20
    6 IF(D-F)1,1,2                                                          BESJ  21
    1 P=((((R8*D+R7)*D+R6)*D+R5)*D+R4)*D = P=(((P+R3)*D+R2)*D+R1)*D+R0      BESJ  22
      BESJ =P/(((D+S2)*D+S1)*D+S0) $ RETURN                                 BESJ  23
    2 IF(D.GT.G) GO TO 9                                                    BESJ  24
      A=ABS(X) $ D=F/D                                                      BESJ  25
      P=((A2*D+A1)*D+A0)/((D+B1)*D+B0)                                      BESJ  26
      Q=  ((C2*D+C1)*D+C0)/(A*((D+D1)*D+D0))                                BESJ  27
      BESJ =(COS(A)*(P+Q)+SIN(A)*(P-Q))/SQRT(A)                             BESJ  28
      RETURN                                                                BESJ  29
    7 IF(D-F)11,11,21                                                       BESJ  30
   11 P=((((((RR7*D+RR6)*D+RR5)*D+RR4)*D+RR3)*D+RR2)*D+RR1)*D+RR0          BESJ  31
      BESJ=X*P/(((D+SS2)*D+SS1)*D+SS0) $ RETURN                             BESJ  32
   21 IF(D.GT.G) GO TO 9                                                    BESJ  33
      A=ABS(X) $ D=F/D                                                      BESJ  34
      P=((AA2*D+AA1)*D+AA0)/((B+BB1)*D+BB0)                                 BESJ  35
      Q=((CC2*D+CC1)*D+CC0)/(A*((D+DD1)*D+DD0))                             BESJ  36
      A=( COS(A)*(Q-P)+SIN(A)*(Q+P))/SQRT(A) $ IF(X.LT.0)A=-A               BESJ  37
      BESJ=A                                                                BESJ  38
      RETURN                                                                BESJ  39
    8 PRINT 81,N                                                            BESJ  40
   81 FORMAT(//15X*ERROR IN BESJ, N =*I5)                                   BESJ  41
      GO TO 100                                                             BESJ  42
    9 PRINT91,X                                                             BESJ  43
   91 FORMAT(//15X*ERROR IN BESJ, ARGUMENT X TOO LARGE. X = *E17.10)        BESJ  44
  100 BESJ=1.E300                                                           BESJ  45
      END                                                                   BESJ  46
```

# APPENDIX C
# COMPUTER PROGRAM FOR EVALUATION OF LOCAL CURRENT DENSITY FOR COPLANAR CONCENTRIC CIRCULAR ELECTRODES UNDER THIN LAYERS OF ELECTROLYTE

```
      ************************************************************************

      PROGRAM THIN1
C
C     THIS PROGRAM COMPUTES THE LOCAL CURRENT DENSITY ALONG THE RADIUS
C     FOR CO-PLANAR, CONCENTRIC, CIRCULAR ELECTRODES COVERED BY
C     A THIN LAYER OF ELECTROLYTE.
C
C     A=RADIUS OF ANODE
C     C=RADIUS OF CATHODE
C     B=THICKNESS OF ELECTROLYTE LAYER
C     L=WAGNER POLARIZATION PARAMETER
C     R=DISTANCE ALONG RADIUS
C     A/C=AR
C     B/C=BR
C     L/C=LR
C     R/C=RR
C     X(N)=NTH ZERO OF BESSEL FUNCTION OF ORDER JORD
C
C     ANODIC AND CATHODIC WAGNER POLARIZATION PARAMETERS ARE EQUAL.
C
      REAL LR,NUM1,NUM2
      DIMENSION X(5000), FACTOR(5000), TERM(5000)
      K=500
C     K=NUMBER OF TERMS IN SUM
      READ 10,AR,BR,LR
   10 FORMAT (3F10.0)
      PRINT 11, AR, BR, LR
   11 FORMAT (1H1,5X,7HAR=A/C= F10.5,5X,7HBR=B/C= F10.5,5X,7HLR=L/C=
     *F10.5,///)
      PRINT 101
  101 FORMAT (26X,*J (XN)*,6X,6HXN*A/C,8X,*J (P)*,8X,*TANH(P)*,4X,
     **(A/C)J (P)*)
      PRINT 102
  102 FORMAT (28X,*0*,25X,*1*,28X,*1*,/)
      PRINT 103
  103 FORMAT (6X,*N*,6X,*X(N)*,9X,*BESSEL2*,9X,*P*,9X,*BESSEL1*,8X,
     **NUM1*,8X,*NUM2*,8X,*DENOM1*,8X,*DENOM2*,7X,*FACTOR(N)*,///)
      JORD=1
      NO=K
      CALL BESZERO(JORD,NO,X)
      DO 20 N=1,K
      P=X(N)*AR
      Q=X(N)*BR
      T=X(N)*LR
      SINHQ=(EXP(Q)-EXP(-Q))/2.0
      COSHQ=(EXP(Q)+EXP(-Q))/2.0
```

```
      TANHQ=SINHQ/COSHQ
      NUM1=TANHQ
      DENOM1=1.0 + (T*TANHQ)
      BESSEL1=BESJ(P,1)
      BESSEL2=BESJ(X(N),0)
      NUM2=AR*BESSEL1
      DENOM2=BESSEL2**2
      FACTOR(N)=(NUM1*NUM2)/(DENOM1*DENOM2)
      PRINT 19,N,X(N),BESSEL2,P,BESSEL1,NUM1,NUM2,DENOM1,DENOM2,FACTOR(N
     *)
   19 FORMAT (3X,I4,1X,E12.5,4(3X,F10.5),4(1X,E13.5))
   20 CONTINUE
      READ 201,RR,DELTA,RCUT
  201 FORMAT (3F10.0)
   21 PRINT 22,RR
   22 FORMAT (///3X,*RR= *F5.3///)
      PRINT 221
  221 FORMAT (25X,8HX(N)*R/C,7X,*J (W)*)
      PRINT 222
  222 FORMAT (41X,*0*,/)
      PRINT 223
  223 FORMAT (6X,*N*,7X,*X(N)*,11X,*W*,9X,*BESSEL3*,6X,*FACTOR(N)*,8X,
     **TERM(N)*,11X,*SUM*,///)
      SUM=0.0
      DO 30 N=1,K
      W=X(N)*RR
      BESSEL3=BESJ(W,0)
      TERM(N)=FACTOR(N)*BESSEL3
      SUM=SUM+TERM(N)
      PRINT 29,N,X(N),W,BESSEL3,FACTOR(N),TERM(N),SUM
   29 FORMAT (3X,I4,1X,E12.5,2(3X,F10.5),3(3X,E13.5))
   30 CONTINUE
      RR=RR + DELTA
      IF (RR.LE.RCUT) GO TO 21
   99 END
```

---

SUBROUTINE BESZERO(JORD,NO,ZERO) AND FUNCTION BESJ(X,N) ARE GIVEN IN APPENDIX B.